

Article

Open Access

# Pan-retinal ganglion cell markers in mice, rats, and rhesus macaques

Francisco M. Nadal-Nicolás<sup>1,2,3,#</sup>, Caridad Galindo-Romero<sup>1,2,#</sup>, Fernando Lucas-Ruiz<sup>1,2</sup>, Nicholas Marsh-Amstrong<sup>4</sup>, Wei Li<sup>3</sup>, Manuel Vidal-Sanz<sup>1,2,\*</sup>, Marta Agudo-Barriso<sup>1,2,\*</sup>

<sup>1</sup> Grupo de Oftalmología Experimental, Instituto Murciano de Investigación Biosanitaria Pascual Parrilla (IMIB), Murcia 30120, Spain

<sup>2</sup> Dpto. Oftalmología, Facultad de Medicina, Universidad de Murcia, Murcia 30120, Spain

<sup>3</sup> Retinal Neurophysiology Section, National Eye Institute, National Institutes of Health, Bethesda, Maryland 20892-2510, USA

<sup>4</sup> Department of Ophthalmology and Vision Science, University of California, Davis, CA 95817, USA

## ABSTRACT

Univocal identification of retinal ganglion cells (RGCs) is an essential prerequisite for studying their degeneration and neuroprotection. Before the advent of phenotypic markers, RGCs were normally identified using retrograde tracing of retinorecipient areas. This is an invasive technique, and its use is precluded in higher mammals such as monkeys. In the past decade, several RGC markers have been described. Here, we reviewed and analyzed the specificity of nine markers used to identify all or most RGCs, i.e., pan-RGC markers, in rats, mice, and macaques. The best markers in the three species in terms of specificity, proportion of RGCs labeled, and indicators of viability were BRN3A, expressed by vision-forming RGCs, and RBPMS, expressed by vision- and non-vision-forming RGCs. NEUN, often used to identify RGCs, was expressed by non-RGCs in the ganglion cell layer, and therefore was not RGC-specific.  $\gamma$ -SYN, TUJ1, and NF-L labeled the RGC axons, which impaired the detection of their somas in the central retina but would be good for studying RGC morphology. In rats, TUJ1 and NF-L

were also expressed by non-RGCs. BM88, ERR $\beta$ , and PGP9.5 are rarely used as markers, but they identified most RGCs in the rats and macaques and ERR $\beta$  in mice. However, PGP9.5 was also expressed by non-RGCs in rats and macaques and BM88 and ERR $\beta$  were not suitable markers of viability.

**Keywords:** RGC; Optic nerve crush; BM88; BRN3A; Estrogen-related receptor  $\beta$ ; ERR $\beta$ ; NEUN; Neurofilament-L; PGP9.5; RBPMS;  $\gamma$ -SYN;  $\beta$ III-tubulin; TUJ1

## INTRODUCTION

In his work “La retina de los vertebrados” (1893), Nobel Prize winner Santiago Ramón y Cajal summarized why the retina is an excellent model for studying neurodegeneration: “its accessibility, its orderly organization in alternate layers of cell

Received: 23 September 2022; Accepted: 13 December 2022; Online: 16 December 2022

Foundation items: This study was supported by the Spanish Ministry of Economy and Competitiveness (PID2019-106498GB-I0), Instituto de Salud Carlos III, Fondo Europeo de Desarrollo Regional “Una manera de hacer Europa” (PI19/00071), Fundación Séneca, Agencia de Ciencia y Tecnología Región de Murcia (19881/GERM/15), Spanish Ministry of Science and Innovation (PID 2019-106498 GB-I00), and Intramural Research Program of the National Eye Institute, National Institutes of Health (NIH/NEI RO1 EY029087)

#Authors contributed equally to this work

\*Corresponding authors, E-mail: manuel.vidal@um.es; martabar@um.es

This is an open-access article distributed under the terms of the Creative Commons Attribution Non-Commercial License (<http://creativecommons.org/licenses/by-nc/4.0/>), which permits unrestricted non-commercial use, distribution, and reproduction in any medium, provided the original work is properly cited.

Copyright ©2023 Editorial Office of Zoological Research, Kunming Institute of Zoology, Chinese Academy of Sciences

bodies and intercellular contacts, and the easy identification of the main direction of the nervous message flow" (Cuenca & de la Villa, 2021). Indeed, the retina offers several advantages over other parts of the central nervous system (CNS), notably: (i) ocular surfaces are transparent, which allows longitudinal studies *in vivo* with non-invasive techniques to track morphological and functional changes in the retina; (ii) treatments, whether cells or drugs, can be administered intravitreally or subretinally, thus avoiding possible systemic adverse effects; (iii) systemic treatments are feasible if the drug crosses the blood-retina barrier; (iv) behavioral analyses are available to test the reach of functional and anatomical improvement; and (v) well-established models of retinal degeneration and disease are available in rats and mice (García-Ayuso et al., 2019a, 2019b; Parrilla-Reverter et al., 2009; Vidal-Sanz et al., 2012, 2017), as well as in other species such as pigs, ground squirrels, and rabbits (Sasaoka et al., 2006; Völggi & Bloomfield, 2002; Xiao et al., 2021); and vi: new therapies may be extrapolated to the rest of the CNS.

The innermost part of the retina contains heterogeneous populations of retinal ganglion cells (RGCs), which are the only projecting neurons in the retina. Their axons form the optic nerve and transmit light-triggered visual and non-visual information to the brain, which elicits corresponding image and non-image responses (Kim et al., 2021; Sanes & Masland, 2015). Unmyelinated RGC axons exit the retina and become myelinated in the optic nerve. During travel, they decussate at the optic chiasm to reach and synapse at several retinorecipient brain areas (Giolli & Towns, 1980; Rodieck, 1979; Schiller, 1986). In rats and mice, more than 90% of RGC axons cross the optic chiasm and, after sending collaterals to various visual nuclei, finally synapse at the contralateral superior colliculi (SCi) (Linden & Perry, 1983; Nadal-Nicolás et al., 2014, 2015b; Salinas-Navarro et al., 2009a, 2009b).

Mammalian models of RGC degeneration can be applied to study retinal diseases (e.g., glaucoma) and unravel how CNS neurons respond to a given insult or systemic disease (e.g., diabetes, sepsis). These models can be inherited, such as mouse strains that develop ocular hypertension with age (De Lara et al., 2014; Liu et al., 2020; Raymond et al., 2009), or induced (Gallego-Ortega et al., 2020; Valiente-Soriano et al., 2015; Vidal-Sanz et al., 2012), including well-characterized models such as axonal trauma (Kalesnykas et al., 2012; Nadal-Nicolás et al., 2009; Parrilla-Reverter et al., 2009; Sánchez-Migallón et al., 2016; Villegas-Pérez et al., 1993), excitotoxicity (Chidlow & Osborne, 2003; Galindo-Romero et al., 2016, transient ischemia (López-Herrera et al., 2002; Sellés-Navarro et al., 1996), and acute or chronic ocular hypertension (Gallego-Ortega et al., 2020; Salinas-Navarro et al., 2010; Valiente-Soriano et al., 2015; Vidal-Sanz et al., 2012, 2015).

RGCs can be divided into several subtypes depending on morphological (~35, Bae et al., 2018), physiological (~30, Baden et al., 2016), or gene expression profiles (~46, Rheume et al., 2018; Tran et al., 2019). They can also be comprehensively grouped based on functional type: i.e., vision-forming and non-vision-forming RGCs. Vision-forming RGCs account for the vast majority (>90% of the total RGC

population in rodents (Galindo-Romero et al., 2013a; Nadal-Nicolás et al., 2009; Salinas-Navarro et al., 2009a, 2009b)) and convey image features to the brain (e.g., color, contrast, movement (Kim et al., 2021; Sanes & Masland, 2015)). Non-vision-forming RGCs (<10% of all RGCs in rodents (Galindo-Romero et al., 2013a; Valiente-Soriano et al., 2014)) are also known as intrinsically photosensitive RGCs (ipRGCs). These RGCs perceive light intensity and regulate circadian rhythm and pupillary reflex (Berg et al., 2019; Provencio et al., 2000), with additional involvement in pattern vision (Ecker et al., 2010; Hattar et al., 2006; Schmidt et al., 2011). These two RGC populations differ in their resilience to injury (Nadal-Nicolás et al., 2015a; Sánchez-Migallón et al., 2018a), and thus merit simultaneous and separate study to dissect the complexities of injury resistance and vulnerability, with the goal of increasing or blocking them, respectively.

In the last two decades, several phenotypic markers of RGCs have been reported, notably BRN3A and RBPMS (Galindo-Romero et al., 2011; Kwong et al., 2010; Nadal-Nicolás et al., 2009; Rodriguez et al., 2014), although others also exist. Because each marker protein has a specific function and expression pattern, optimal proteins must be selected based on their properties and what is being assessed (e.g., RGC morphology, axonal structure, or viability).

In the current review, we focus on those markers used to detect all (or most) RGCs, i.e., pan-RGC markers. Subtype-specific RGC markers have been reviewed elsewhere (Corral-Domenge et al., 2022; Tapia et al., 2022). This review does not include markers for ipRGCs, as they are typically immunoidentified based on their expression of melanopsin, the pigment that renders them photosensitive (Provencio et al., 2000). This protein is expressed at varying levels depending on the ipRGC subtype, with low-expressing M4–M6 subtypes showing lower detection sensitivity than standard fluorescence microscopy (Berg et al., 2019). Nevertheless, melanopsin immunodetection is the most common approach used to identify ipRGCs, subsequently named melanopsin<sup>+</sup> RGCs (m<sup>+</sup> RGCs). These m<sup>+</sup> RGCs also express pan-RGC markers, but relatively heterogeneously (Chen et al., 2021; Jain et al., 2012; Karnas et al., 2013; Tran et al., 2019); for example, some, such as BRNB, are expressed in a subpopulation of m<sup>+</sup> RGCs (Nadal-Nicolás et al., 2012); others, such as RBPMS, are expressed in all m<sup>+</sup> RGCs (Rodriguez et al., 2014); and some, such as THY-1 and BRN3A, are not expressed in any (Barnstable & Dräger, 1984; Galindo-Romero et al., 2011; Grillo & Stella, 2018; Nadal-Nicolás et al., 2014). The latter situation presents some advantages, as discussed below.

## Methods to identify RGCs

**Hematoxylin/eosin (H&E) staining:** H&E staining has been used to stain the retina and identify cells in the ganglion cell layer (GCL) where RGCs lie (Sasaoka et al., 2006). However, identification of these neurons may not be accurate, as there is an equally abundant population of displaced amacrine cells in this layer (Nadal-Nicolás et al., 2015c).

**Quantification of optic nerve axons:** Quantification of RGC axons in electron microscopy images from optic nerve

sections is a common, albeit indirect, approach for assessing RGC numbers (Jeon et al., 1998; Sefton & Lam, 1984). Today, axonal quantification is seldom used for this purpose but is the assay of choice for assessing RGC regeneration using anterograde tracers or immunodetection of proteins expressed in regenerating axons (Avilés-Trigueros et al., 2000; Bollaerts et al., 2018; Norte-Muñoz et al., 2021).

**Retrograde tracing:** An advance from H&E staining is the use of retrograde tracers placed in retinorecipient areas or around the optic nerve (Lafuente et al., 2002; Nadal-Nicolás et al., 2015b; Thanos et al., 1987; Vidal-Sanz et al., 1988), which are then transported from the axonal terminals or optic nerve axons to RGC somas in the retina.

Retrograde tracing can be conducted with passively or actively transported tracers. Passive tracers, such as rhodamine isothiocyanate (RITC), are placed on the optic nerve stump and are transported to the RGC somas with no energy requirement. The main disadvantages of these tracers are that RGCs are axotomized and the dye can reach the eye, thus staining the retina non-specifically. Active tracers, such as fluorogold (FG) and hydroxystilbamidine methanesulfonate (OHSt), require energy for transport and can be applied to the intact optic nerve or main retinorecipient areas (SCi in rodents) without causing RGC death (Nadal-Nicolás et al., 2015a, 2015b). Tracing from the SCi can be accomplished by stereotaxic injection or by exposing both (or one) SCi and applying the tracer to their surface. This latter method is highly reliable and reproducible. Tracing from the SCi provides a very good signal and RGCs are uniformly labeled, although the 2%–3% of RGCs that do not project to the SCi are not traced, whereas when the tracer is wrapped around the optic nerve, all retinofugal projections are traced but the optic nerve head is brightly labeled (Nadal-Nicolás et al., 2015b).

Actively transported tracers identify RGCs precisely; however, when traced RGCs die, they are phagocytized by microglial cells, which in turn are transcellularly labeled (Thanos et al., 1987). This may be an advantage if the purpose is to study microglial activation and phagocytic status (Galindo-Romero et al., 2013b), but not to study the course of RGC death, for two reasons: (i) transcellularly labeled microglial cells must be distinguished from traced RGCs and this cannot (yet) be done automatically; and (ii) dead RGCs disappear from the tissue upon phagocytosis, which takes some time. For example, there is a delay of 3 days between RGC death and tissue clearance in rats (Nadal-Nicolás et al., 2017). For most neuroprotection studies, this is of little importance because, although quantification of the traced RGCs suggests that the course of RGC death is slower than it actually is, it is proportional between the control and treated groups. However, this artefact becomes an issue when testing anti-inflammatory or microglial-modulating therapies: notably, RGCs would appear to survive if microglial cells are inactivated or depleted, but what remain are tracer-filled corpses. In this scenario, tracing is not a suitable approach to assess RGC survival.

There are other considerations when deciding to use tracing. First, this invasive method must be performed several days before euthanasia and involves either exposing the optic nerve or performing craniotomy or stereotaxis to reach the

areas with the highest RGC projection (Nadal-Nicolás et al., 2015b; Salinas-Navarro et al., 2009a, 2009b), which in rodents, but not in all species, is the SCi. These characteristics preclude the use of tracers in highly evolved species, such as primates. Second, tracing alters gene expression in RGCs (Nadal-Nicolás et al., 2015a) and may affect their functional properties. Finally, after retinal permeabilization for immunodetection, tracers may diffuse, thereby staining the tissue and losing their somatic signal, which is especially pronounced for passively transported tracers.

**Phenotypic markers:** Phenotypic RGC markers are those proteins or RNAs expressed only by RGCs in the retina, either as whole populations or specific functional or physiological subtypes (Corral-Domenge et al., 2022; Kay et al., 2011; Rheume et al., 2018; Tapia et al., 2022). Several transgenic mouse strains carry a reporter under the promoter of certain markers, such as Thy-1 (Iaboni et al., 2020; Munaut et al., 2001; Raymond et al., 2009). In some cases, the penetrance of these transgenes is incomplete, and thus the RGCs are sparsely labeled, which is useful for morphologically clustering RGCs or tracking individual RGCs *in vivo* (Badea & Nathans, 2011; Hayworth et al., 2008; Iaboni et al., 2020; Simmons et al., 2016). However, most laboratories do not have access to these strains, so immunohistofluorescence is usually used to detect these markers, although *in situ* hybridization is also feasible (Surgucheva et al., 2008).

The advantages of immunodetection are clear: i.e., no previous animal manipulation is required, the technique is relatively easy, and most antibodies are commercially available and relatively affordable, thus within the means of most groups.

#### **When is an RGC marker a good marker of RGCs?**

The answer to the above question depends on what we are looking for. If the goal is to identify all RGCs, the marker should be expressed by all or at least most RGCs. To study morphology, markers expressed throughout the entire RGC (axons, dendrites, and cytoplasm) are ideal, whereas nuclear or cytoplasmic markers exhibit better performance for quantification.

In all cases, however, three simple rules apply: (1) The marker must be specific and its expression in the retina or at least in the GCL must be restricted to RGCs. (2) The marker must not change its expression pattern after injury. (3) The marker must be a viability marker, and its expression must decline as the RGC dies. This is particularly important when performing survival and neuroprotection assays.

#### **Pan-RGC markers**

Thy-1 was one of the earliest described RGC-specific antigens, with expression found in most RGCs (Barnstable & Dräger, 1984). However, its use as a tool to identify RGCs declined when its expression pattern was found to change after retinal injury (Chidlow et al., 2005; Dabin & Barnstable, 1995) and its down-regulation was faster than actual loss of RGCs (Huang et al., 2006; Schlamp et al., 2001). This was elegantly demonstrated using *Bax*<sup>-/-</sup> mice whose RGCs were resistant to axotomy-induced death (Li et al., 2000; Schlamp

et al., 2001). In that study, Thy-1 expression decreased in the axotomized retina despite the survival of RGCs, suggesting that down-regulation preceded a committed step in the apoptotic program of the cells. As such, Thy-1 was not included in our review.

Here, we analyze and discuss gold standard (RBPMS and BRN3A), commonly used (NEUN, NF-L,  $\gamma$ -SYN, and TUJ1), and lesser-known RGC markers (BM88, ERR $\beta$ , and PGP9.5). We first review current literature regarding each marker (in alphabetical order) and then compare their expression patterns, specificities, and accuracy in rats (*Rattus norvegicus*, albino Sprague Dawley strain), mice (*Mus musculus*, pigmented C57BL/6J strain), and rhesus macaques (*Macaca mulatta*).

**BM88** or CEND1 (cell cycle exit and neuronal differentiation protein 1) is a neuronal lineage-specific regulator that induces cell cycle exit and neuronal differentiation and maturation (Katsimpardi et al., 2008; Koutmani et al., 2004; Wakabayashi et al., 2010). It was originally described as an RGC marker in rats and cats in 1996 (Siddiqui et al., 2014; Wakabayashi et al., 1996a, 1996b) and in ferrets several years later (Quan et al., 1999). BM88 is expressed in the somas and axonal bundles of 94%–100% of RGCs traced from the superior colliculus, depending on their retinal eccentricity (Wakabayashi et al., 1996b). Early after optic nerve injury in rats, its expression per neuron increases compared with intact RGCs, but then decreases as RGC death progresses (Siddiqui et al., 2014). This down-regulation is faster than the loss of traced RGCs, suggesting that BM88 is not a good RGC marker. However, as mentioned earlier, RGC death and clearance are not parallel, and down-regulation of BM88 may be in accordance with RGC death, i.e., BM88 is a marker of RGC viability.

**BRN3A** (brain-specific homeobox/POU domain protein 3A) belongs to the POU-IV class of neural transcription factors together with BRN3B and BRN3C. These proteins play important roles during development, orchestrating the differentiation, specification, and axonal elongation of RGCs (Ávila-García et al., 2012; Badea & Nathans, 2011; Ghinia et al., 2019; Hirsch & Harris, 1997; Liu et al., 2000; Muzyka et al., 2018; Pan et al., 2005; Parmhans et al., 2021; Plaza et al., 1999; Sajgo et al., 2017; Xiang et al., 1995) and other somatosensory neurons (Huang et al., 2001; Latchman et al., 1992; Xiang et al., 1995). They are conserved across phylogeny and perform similar functions from invertebrates (orthologs UNC-86 in *Caenorhabditis elegans* or Acj-6 in *Drosophila*) to vertebrates (Brn3), initiating and maintaining neuronal identity (reviewed in Leyva-Díaz et al., 2020; Serrano-Saiz et al., 2018).

BRN3A expression in adult RGCs has been described in fish (Sato et al., 2007), birds (chickens and pigeons, Galindo-Romero et al., 2016; Sheng et al., 2021), and mammals (mice, rats, cats, ground squirrels, humans, monkeys, pigs, dogs, alpacas, and blind moles, Ávila-García et al., 2012; Bouskila et al., 2020; Esquivá et al., 2016; Galindo-Romero et al., 2011; Kim et al., 2006; Nadal-Nicolás et al., 2009; Ruzafa et al., 2017; Wang et al., 2015; Xiang et al., 1995; Xiao et al., 2021; Zhang et al., 2010).

BRN3A is also involved in neuronal survival by activating

pro-survival genes and inhibiting pro-apoptotic genes (Budram-Mahadeo et al., 2002; Farooqui-Kabir et al., 2004; Hudson et al., 2016; Serrano-Saiz et al., 2018; Smith et al., 1998). In the retina, BRN3A expression is reduced as RGCs undergo apoptosis (Sánchez-Migallón et al., 2016), suggesting that BRN3A is a viability marker. In rats and mice, BRN3A is expressed in vision-forming RGCs but not in m<sup>+</sup> RGCs (Chen et al., 2011; Galindo-Romero et al., 2013a; Nadal-Nicolás et al., 2012, 2014; Sánchez-Migallón et al., 2016, 2018a; Valiente-Soriano et al., 2014), making this marker ideal for studying two populations in parallel but separately.

These properties, together with its nuclear expression that simplifies RGC quantification, are why BRN3A has become a gold standard for identifying RGCs.

**ERR- $\beta$**  (estrogen-related receptor beta or steroid hormone receptor ERR2) is an orphan nuclear hormone receptor that does not respond to natural estrogen ligands such as estradiol. Little is known about the role and expression patterns of ERR- $\beta$  in the CNS. Real et al. (2008) reported that ERR- $\beta$  is expressed in all retinorecipient nuclei, as well as in projecting RGCs, although to what extent is unknown. ERR- $\beta$  is also expressed in photoreceptors in the retina (Kunst et al., 2015) and plays a major role in rod survival (Onishi et al., 2010).

**NF-L** (neurofilament light polypeptide), together with NF-M (medium) and NF-H (high), forms part of the neuronal intermediate neurofilament triplet. The neurofilament triplet assembles in the neuronal soma and travels down the axon via slow axonal transport, a process that relies on phosphorylation (Black & Lasek, 1980; Hoffman & Lasek, 1975; Jung et al., 2000; Nixon et al., 1989). NFs are found in somatic dendrites or axonal compartments depending on their phosphorylation state (Dräger & Hofbauer, 1984; García-Ayuso et al., 2019b; Parrilla-Reverter et al., 2009; Ruiz-Ederra et al., 2004; Sánchez-Migallón et al., 2018b; Triplett et al., 2014; Vickers et al., 1994). In the mammalian retina, NFs are expressed in RGCs, but are also expressed in horizontal cells (e.g., rats, mice, and guinea pigs), bipolar cells (e.g., rabbits and guinea pigs, Kong & Cho, 1999; Raymond et al., 2009; Ruiz-Ederra et al., 2004; Vickers & Costa, 1992), and an amacrine cell subtype (e.g., rabbits and cats, Gábel & Straznicky, 1992; Völgyi & Bloomfield, 2002).

Differential phosphorylation of these structural proteins is useful for the selective recognition of RGC somas (Feng et al., 2013; Lin et al., 2018; Raymond et al., 2009) or their intraretinal axons, and for the identification of degenerating RGCs, which aberrantly express highly phosphorylated isoforms in their cytoplasm (García-Ayuso et al., 2019b; Parrilla-Reverter et al., 2009; Sánchez-Migallón et al., 2018b).

NF-L is expressed by most RGCs in pigs, humans (Ruiz-Ederra et al., 2004), and hamsters (Kong & Cho, 1999) and has been used to assess RGCs in rabbits (Nixon et al., 1989), mice (Mali et al., 2005; Raymond et al., 2008), and rats (Chidlow et al., 2005; Chidlow & Osborne, 2003). To the best of our knowledge, however, the proportion of NF-L<sup>+</sup> RGCs in the three species analyzed here has not yet been reported.

**NEUN/Rbfox3** (neuronal nuclei antigen, RNA binding protein fox-1 homolog 3) was first described in 1992 (Mullen et al.,

1992) as a nuclear marker of postmitotic neurons in mammals, birds, and reptiles, although it shows perinuclear and cytoplasmic expression in some neuronal populations (Van Nassauw et al., 2005, reviewed in Gusef'nikova & Korzhvskiy, 2015).

NEUN is a member of the Fox1 gene family of splicing factors and contains several isoforms (from 40 to 50 kDa), which are predominantly, but not exclusively, located in the nuclei (Kim et al., 2009). This protein plays an essential role in neuronal development, maturation, and specificity, and regulates neurogenesis and synaptogenesis (Kim et al., 2013; Lin et al., 2018).

NEUN is expressed by most central and peripheral neurons, except for populations such as Purkinje cells, photoreceptors, and olfactory bulb mitral cells (Mullen et al., 1992). In the mammalian retina, NEUN is expressed in RGCs, displaced amacrine cells, and horizontal cells (Buckingham et al., 2008; Johansson et al., 2010; Lin et al., 2018; Mullen et al., 1992; Rodriguez et al., 2014; Telegina et al., 2019). NEUN expression in displaced amacrine cells has been reported in pigs (Johansson et al., 2010) and mice (Lin et al., 2018). Although it is expressed in amacrine cells, several groups have used it as an RGC-specific marker (Buckingham et al., 2008).

Because NEUN is expressed in RGCs and is important for neuronal specificity, Lin et al. (2018) studied its role in visual function and found it to be dispensable. Thus, despite its important role as a splicing regulator, its deficiency does not affect RGC functionality.

NEUN is also expressed in cultured human and rodent astrocytes (Darlington et al., 2008), and its down-regulation after cerebral ischemia is not correlated with neuronal death (Ünal-Çevik et al., 2004).

**PGP9.5** (ubiquitin carboxyl-terminal hydrolase isozyme L1 - UCHL1-, neuron cytoplasmic protein 9.5, or protein gene product 9.5) is a ubiquitin carboxy-terminal hydrolase and ligase, recycling ubiquitin from degraded proteins and tagging proteins with ubiquitin for degradation (Setsue & Wada, 2007). It also plays a role in neurogenesis and apoptosis, oxidative stress protection, and synaptic plasticity (Gong & Leznik, 2007; Harada et al., 2004; Lansbury, 2006). PGP9.5 is highly abundant, constituting around 1%–2% of soluble proteins in the brain, and is primarily expressed in neurons (Day, 1992; Trowern et al., 1996; Wilkinson et al., 1992), although can also be found outside the CNS in carcinomas and other mesodermal tissues (Jara et al., 2013; Matuszczak et al., 2020).

Retinal PGP9.5 expression was first reported in bovines in the late 1990s (Piccinini et al., 1996) and later in cats (May et al., 2005) and other mammals (Esteve-Rudd et al., 2010). Esteve-Rudd et al. (2010) found that PGP9.5 is expressed in RGC somas and their axons, as well as in amacrine, bipolar, and horizontal cells and cones of several mammals, but not in rodents.

Given its role in protein ubiquitination, PGP9.5 is thought to play an important role in the degradation of abnormal protein deposits found in neurodegenerative diseases (Gong & Leznik, 2007; Wilkinson et al., 1992). Indeed, in rodent models of glaucoma, PGP9.5 expression is reduced in the retina and

optic nerve, thereby increasing levels of proapoptotic proteins that would otherwise be degraded by the proteasome, thus amplifying neuronal death and disease progression (Dibas et al., 2008).

RBPMS (RNA-binding protein with multiple slicing or Hermes) was first described during embryonic heart development in frogs (Gerber et al., 1999). Hermes belongs to the largest family of RNA-binding proteins, i.e., RNA recognition motif (RRM) family, hence its name (HEart, RRM expressed sequence).

**RBPMS** is a transcriptional activator of the TGF- $\beta$ 1/Smad pathway, a pleiotropic signaling pathway whose dysregulation is associated with several peripheral diseases (Gordon & Blobel, 2008).

RBPMS expression in the retina was first observed in frogs (Gerber et al., 1999), with its use as an RGC marker described some 11 years later (Kwong et al., 2010). Subsequent studies investigated RGC degeneration models (Kwong et al., 2011) and characterized RBPMS in other mammalian species, such as guinea pigs, monkeys, mice (Rodriguez et al., 2014), cats (Wang et al., 2016), blind moles (Esquivá et al., 2016), pigs, humans (Pereiro et al., 2020), and ground squirrels (Xiao et al., 2021).

The expression pattern of RBPMS in the retina, which is somatic under physiological states, changes under hypoxic conditions and localizes to RGC dendrites in the inner plexiform layer (IPL) (Pereiro et al., 2020), consistent with the fact that hypoxic insults activate the TGF- $\beta$ 1 pathway (Xu et al., 2018). In frog RGCs, RBPMS influences axonal and synaptic biology (Hörnberg et al., 2013).

RBPMS labels vision and non-vision forming RGCs. Thus, it has become a gold standard for identifying RGCs, regardless of their functional subtypes, although it may also label a small proportion of GABA<sup>+</sup> displaced amacrine cells (dACs; Rodriguez et al., 2014).

**$\gamma$ -SYN** (gamma synuclein or Persyn) is a cytoskeleton-associated protein that maintains neurofilament integrity and axonal architecture. While it is highly abundant in the brain, it is also found in other tissues, such as muscle, intestine, and kidneys. Studies have shown that  $\gamma$ -SYN levels are elevated in some cancers (Takemura et al., 2021) and in the cerebrospinal fluid of patients with Alzheimer's disease (Nilsson et al., 2021), thus potentially serving as a biomarker of cancer and Alzheimer's progression.

Specific  $\gamma$ -SYN expression in RGCs was first described in mice (Mu et al., 2004), then later described as a marker of RGCs in humans (Surgucheva et al., 2008), mice (Buckingham et al., 2008), and macaques (Hirata et al., 2015), although it is also expressed in some horizontal cells, presumably those with longer axons. In the retina,  $\gamma$ -SYN expression decreases after optic nerve axotomy and increased ocular hypertension (Liu et al., 2020). Interestingly, it accumulates in the optic nerve upon optic nerve axotomy and plays a role in glial scar formation (Nguyen et al., 2011).

**TUJ1** (neuron-specific class III beta-tubulin, also known as  $\beta$ -tubulin or TUBB3) is a major component of microtubules and is found in neuronal somas, dendrites, and axons. In the retina, it is highly expressed in RGCs in monkeys (Ikeda et al., 2019), birds (Álvarez-Hernán et al., 2020; Romero-Alemán

et al., 2012; Santos et al., 2014), reptiles (Romero-Alemán et al., 2010), and rodents (Zhou et al., 2018). TUJ1 immunodetection can be used to study RGC axonal bundles and to quantify and identify their somas (Miller et al., 2020).

In the second part of this review, we show the expression patterns of the above markers (Figure 1) in rats (Figures 2, 3), mice (Figures 4, 5), and macaques (Figures 6, 7).

## MATERIALS AND METHODS

### Animal handling and ethics statement

Adult female rats (albino Sprague Dawley strain) and mice (pigmented C57BL/6J strain) were kept at the University of Murcia animal housing facilities in temperature- and light-controlled rooms (12 h light/dark cycle) with food and water administered *ad libitum*. All rodent procedures were approved by the Institutional Animal Care and Use Committee at the University of Murcia (Murcia, Spain) and performed according to the guidelines of the institution (approved protocols A13150201, A1320140704, A13170110, and A13170111).

Surgery was carried out under general anesthesia using a mixture of ketamine (60 mg/kg, Ketolar, Spain) and xylazine (10 mg/kg, Rompún, Spain) administered intraperitoneally. Analgesia was provided via subcutaneous administration of buprenorphine (0.1 mg/kg; Buprex (buprenorphine 0.3 mg/mL); Schering-Plough, Spain). During and after anesthesia, ointment (Tobrex, Spain) was added to the eyes to prevent corneal desiccation. Animals were sacrificed with an intraperitoneal injection of an overdose of sodium pentobarbital (Dolethal, Vetoquinol, Spain).

Post-mortem eyes from rhesus macaques (*M. mulatta*, 8–12-years-old,  $n=4$  eyes) were obtained from Dr. Lauren Brinster (DRSB, NIH), Dr. Mark A. Eldridge (NIMH, NIH), and Dr. Julie Mattison and Dr. Kielee Jennings (NHPC-NIA, NIH). The macaque retinas were dissected in accordance with the biosafety policies for the use of non-human primate tissues and fluids at NIH to ensure proper protection (BSL-2).

### Assessment of RGCs

To assess how many RGCs express specific markers in the two murine species, ipsilaterally and contralaterally projecting RGCs were traced by applying FG (rats; Fluorochrome Inc., USA) and OHSt (mice; Molecular Probes, The Netherlands) to the SCI surfaces, following previously published methods

(Nadal-Nicolás et al., 2015b; Salinas-Navarro et al., 2009a, 2009b). We used tracing for RGC baseline for several reasons: first, it is a marker-independent method and we wanted to compare markers; second, using a marker as baseline would not be feasible for all marker combinations due to antibody incompatibilities; and third, only RGCs are traced, allowing evaluation of non-RGCs expressing each marker. However, the shortcoming is that tracing from both SCI labels 98% and 97% of RGCs in rats and mice, respectively. Therefore, a 2%–3% mismatch with immunodetected markers should not be considered significant.

To assess the percentage of RGCs in the GCL and to infer the proportion of intrinsically photosensitive RGCs, RBPMS and BRN3A were immunoidentified together and nuclei were counterstained with 4',6-diamidino-2-phenylindole (DAPI) (Vectashield mounting medium with DAPI, Palex Iberica, Spain).




To investigate the extent to which marker down-regulation was correlated with RGC viability, the expression of each marker was compared to that of BRN3A at 5 days after optic nerve crushing (ONC). ONC was performed as reported previously (Galindo-Romero et al., 2011; Nadal-Nicolás et al., 2009; Sánchez-Migallón et al., 2011) and each marker was immunodetected with BRN3A. After quantification (see below), the percentage of RGCs in the axotomized versus intact retinas was calculated for each marker and BRN3A. If the percentage of marker<sup>+</sup> RGCs was lower than that of BRN3A<sup>+</sup>RGCs, its expression disappeared earlier than that of BRN3A, and vice versa.

RGC death was already evident in both murine species at 5 days post lesion. This loss was visualized by BRN3A immunodetection and retrograde tracing (Galindo-Romero et al., 2011; Nadal-Nicolás et al., 2009; Parrilla-Reverter et al., 2009). RGC loss was observed earlier with BRN3A than with tracing because microglial uptake is slower than actual RGC death, and this shift is more noticeable in rats than mice due to slower microglial activation in the former (Nadal-Nicolás et al., 2017; Vidal-Sanz et al., 2017).

Study and quantification design are shown in Figure 1.

### Quantification

Three species markers were quantified in the central and peripheral retina. Macaque images were taken from the central retina but not the fovea.

	 	
How many RGCs express a marker?	Tracer and marker positive	BRN3A and marker positive
How many non-RGCs express a marker?	Tracer negative and marker positive	BRN3A negative and marker positive
Marker down-regulation after axotomy	BRN3A and marker correlation	
Proportion of ipRGCs	RBPMS positive and BRN3A negative	
Percent of RGCs in the GCL	DAPI <sup>+</sup> nuclei RBPMS positive	
Percent of non-RGCs in the GCL	DAPI <sup>+</sup> nuclei RBPMS negative	

**Figure 1 Analyses performed in three species**

Percentages were relative to traced RGCs in rodents and BRN3A<sup>+</sup> RGCs in macaques (first row), marker<sup>+</sup> cells (second row), all quantified RGCs (third row), RBPMS<sup>+</sup> RGCs (fourth row), and DAPI-stained nuclei (fifth and sixth rows).

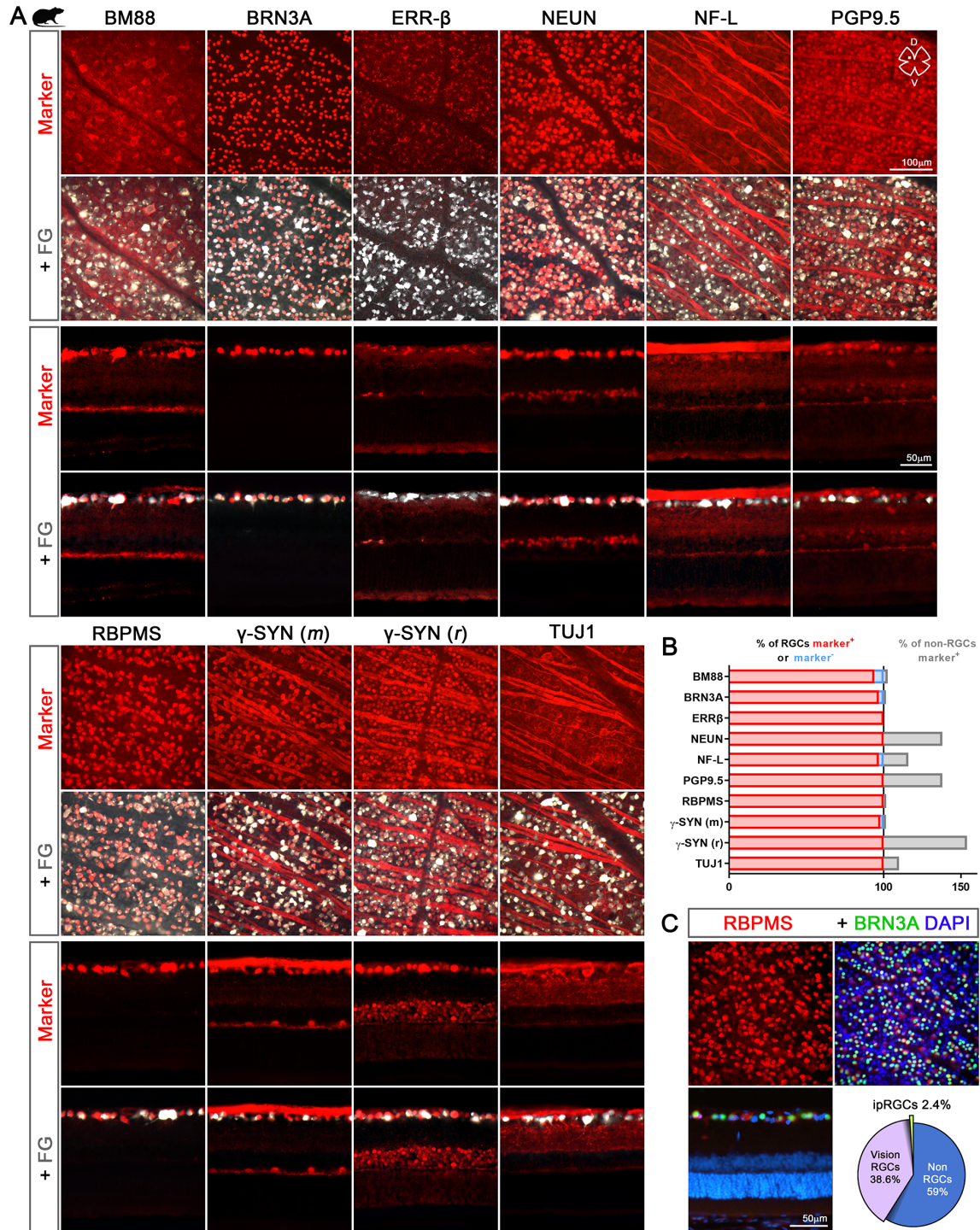


**Figure 2** BM88, BRN3A, ERR-β, NEUN, NF-L, PGP9.5, RBPMS, α-SYN, γ-SYN, and TUJ1 expression in intact rat retina

A: Immunodetection of each marker (red) in retinal flat-mounts and cross-sections and their co-localization with RGCs traced with fluorogold (FG, white) from superior colliculi. γ-SYN was immunodetected with two different primary antibodies, one raised in mice (m) and one in rabbits (r). See text for further explanation. B: Column graphs in red show percentage of RGCs expressing each marker (number of FG<sup>+</sup> marker<sup>+</sup> RGCs over total number of traced RGCs), in blue show percentage of RGCs not expressing the marker (number of FG<sup>+</sup> marker<sup>-</sup> RGCs over total number of traced RGCs), and in gray show percentage of non-RGCs in GCL that express the marker (number of FG<sup>-</sup> marker<sup>+</sup> cells over total number of marker<sup>+</sup> cells). C: Magnifications showing RBPMS and BRN3A immunodetection with DAPI nuclear counterstaining in flat-mounts and cross sections. Bottom-right: part of a whole graph showing percentage of RGCs (purple, vision forming; green, ipRGCs) and non-RGCs (blue) in GCL. DAPI<sup>+</sup> RBPMS<sup>+</sup>: RGCs; DAPI<sup>+</sup> RBPMS<sup>-</sup> cells: non-RGCs (of DAPI<sup>+</sup> nuclei); RBPMS<sup>+</sup>BRN3A<sup>-</sup> cells: ipRGCs (of RBPMS<sup>+</sup> cells). Within 41% of RGCs, 2.4% were estimated as ipRGCs.

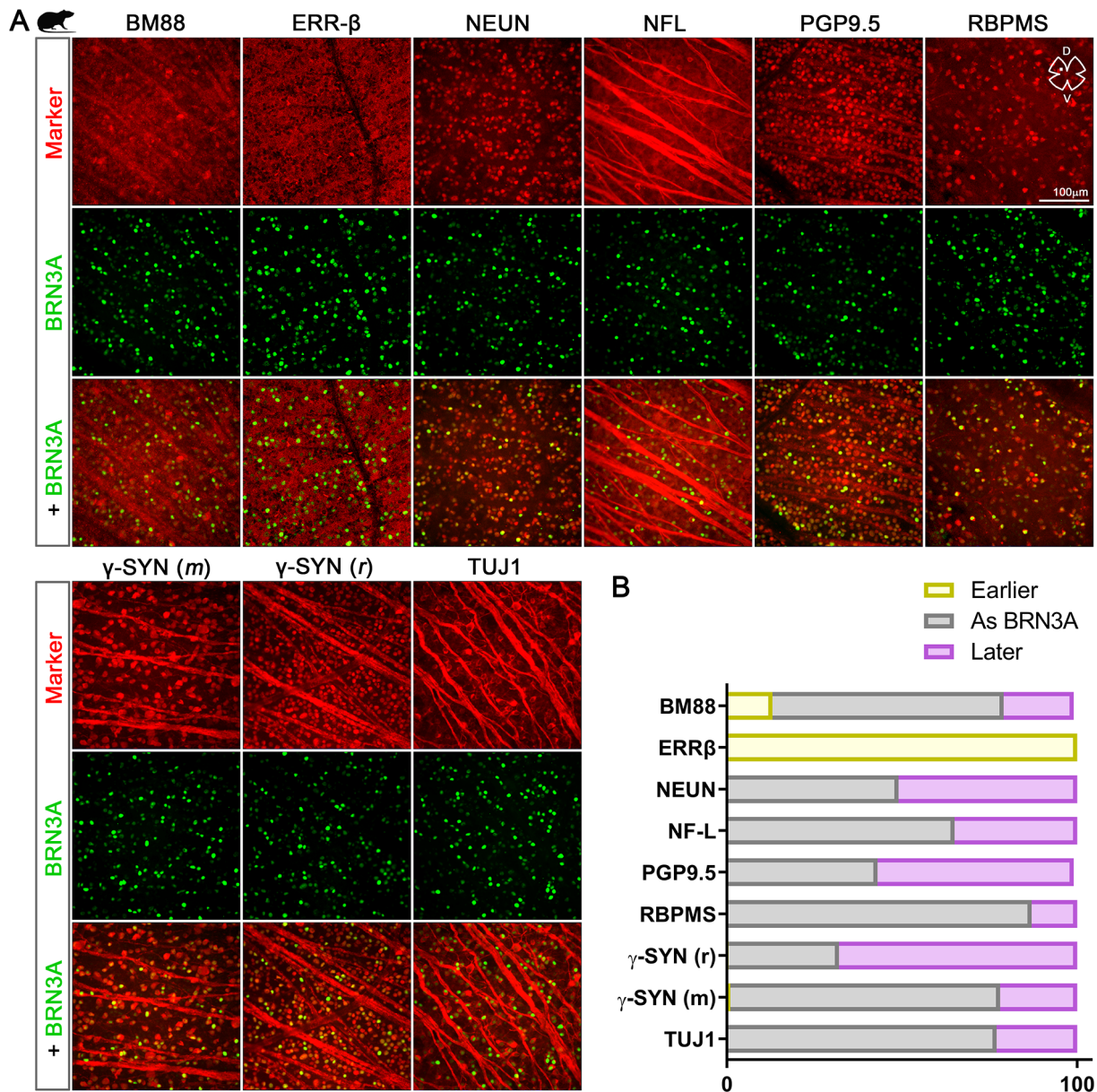


**Figure 3** Marker expression after optic nerve axotomy in rats

A: Double immunodetection of each marker (red) with BRN3A (green) in flat-mounted retinas 5 days after ONC. B: Column graph in yellow shows percentage of RGCs in which marker is down-regulated earlier than BRN3A, in gray shows percentage of RGCs in which BRN3A and marker follow the same regulation, and in purple shows percentage of RGCs in which marker is down-regulated later than BRN3A. 100% is the sum of all quantified cells.

Briefly, in the rats and mice, one image from the center and one from the periphery was acquired per retinal quadrant for each flat-mounted retina ( $n=3$  intact and 3 axotomized retinas per species, analysis, and marker), giving a total of eight frames/retina. Images were acquired at 1.2 and 2.5 mm (rat) or 0.5 and 1 mm (mouse) from the optic nerve head. In macaques, 5–6 images were acquired for each flat-mount ( $n=3$ /marker) at 0.5 and 3.5 mm from the periphery (10–12 frames/retina). Frame size was 0.216 mm<sup>2</sup>, 0.151 mm<sup>2</sup>, and 0.180 mm<sup>2</sup> for mice, rats, and macaques, respectively. For cross-sections ( $n=3$  retinas/species, analysis, and marker), images were taken from samples at 0.5–1.5 mm from the optic

nerve. Quantification was performed manually. First, images acquired from the same area of each analysis (i.e., marker+tracer, marker+RBPMS+DAPI, and marker+BRN3A, see Figure 1) were superimposed in Adobe Photoshop. Next, double- or single-positive cells were dotted with a different color and quantified automatically. DAPI<sup>+</sup> nuclei were also quantified automatically. Images were processed by two experienced investigators and analyses were not blinded because the expression pattern of each protein/tracer is easily recognizable.

Quantification of markers with somatic and axonal expression (NF-L, BM88, PGP9.5, both SYNs and Tuj-1) that



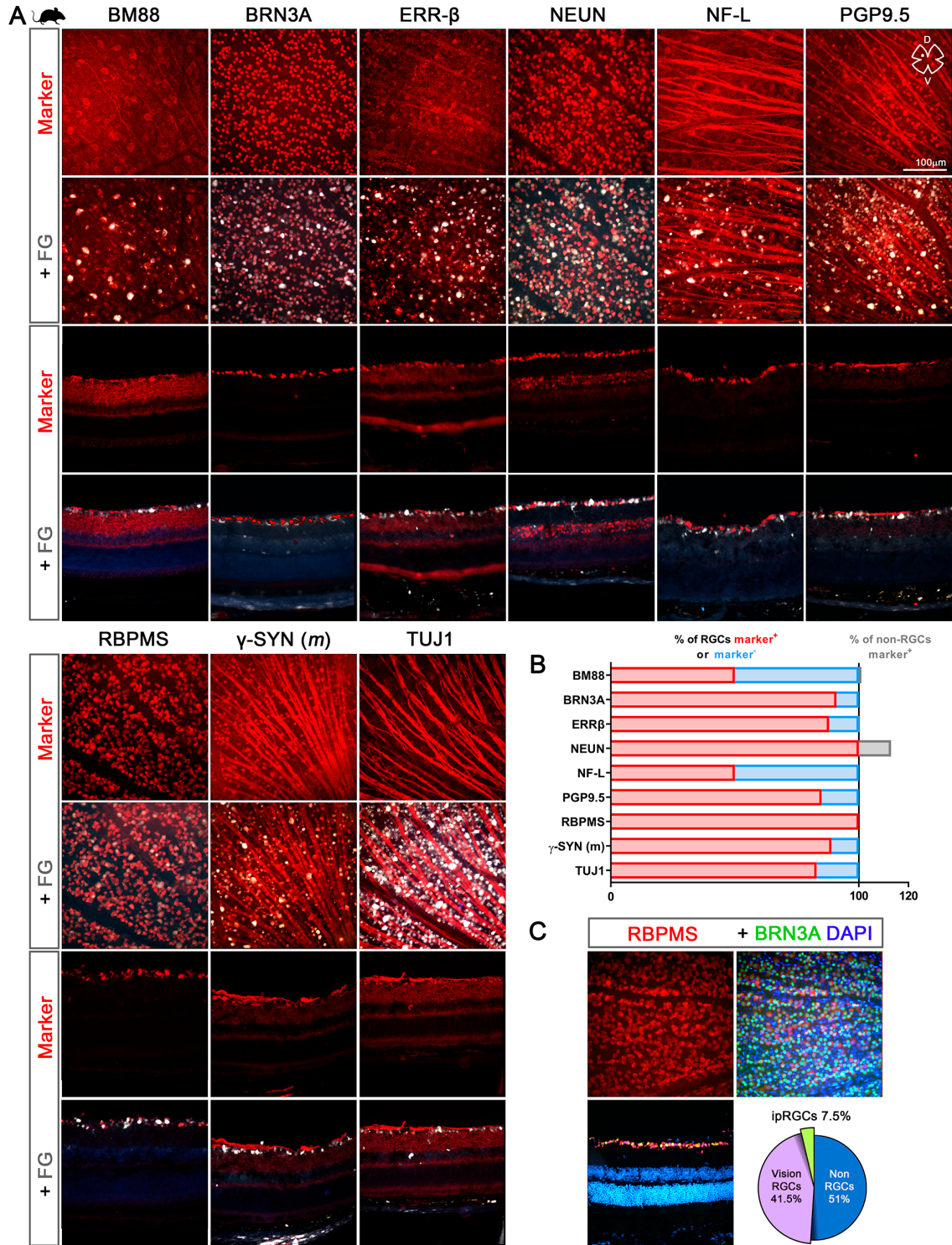


**Figure 4** BM88, BRN3A, ERR- $\beta$ , NEUN NF-L, PGP9.5, RBPMS,  $\gamma$ -SYN, and TUJ1 expression in intact mouse retina

A: Immunodetection of each marker (red) in retinal flat-mounts and cross-sections and their co-localization with RGCs traced with OHSt (white) from superior colliculi. B: Column graphs in red show percentage of RGCs that express each marker (number of OHSt<sup>+</sup> marker<sup>+</sup> RGCs over total number of traced RGCs), in blue show percentage of RGCs that do not express the marker (number of OHSt<sup>+</sup> marker<sup>-</sup> RGCs over total number of traced RGCs), and in gray show percentage of non-RGCs in GCL that express the marker (number of FG<sup>-</sup> marker<sup>+</sup> cells over total number of marker<sup>+</sup> cells). C: Magnifications showing RBPMS and BRN3A immunodetection with DAPI nuclear counterstaining in flat-mounts and cross sections. Bottom-right: part of a whole graph showing percentage of RGCs (purple, vision forming; green, ipRGCs) and non-RGCs (blue). DAPI<sup>+</sup> RBPMS<sup>+</sup>: RGCs; DAPI<sup>+</sup> RBPMS<sup>-</sup> cells: non-RGCs (of DAPI<sup>+</sup> nuclei); RBPMS<sup>+</sup>BRN3A<sup>+</sup> cells: ipRGCs (of RBPMS<sup>+</sup> cells). Within 49% of RGCs, 7.5% were estimated as ipRGCs.

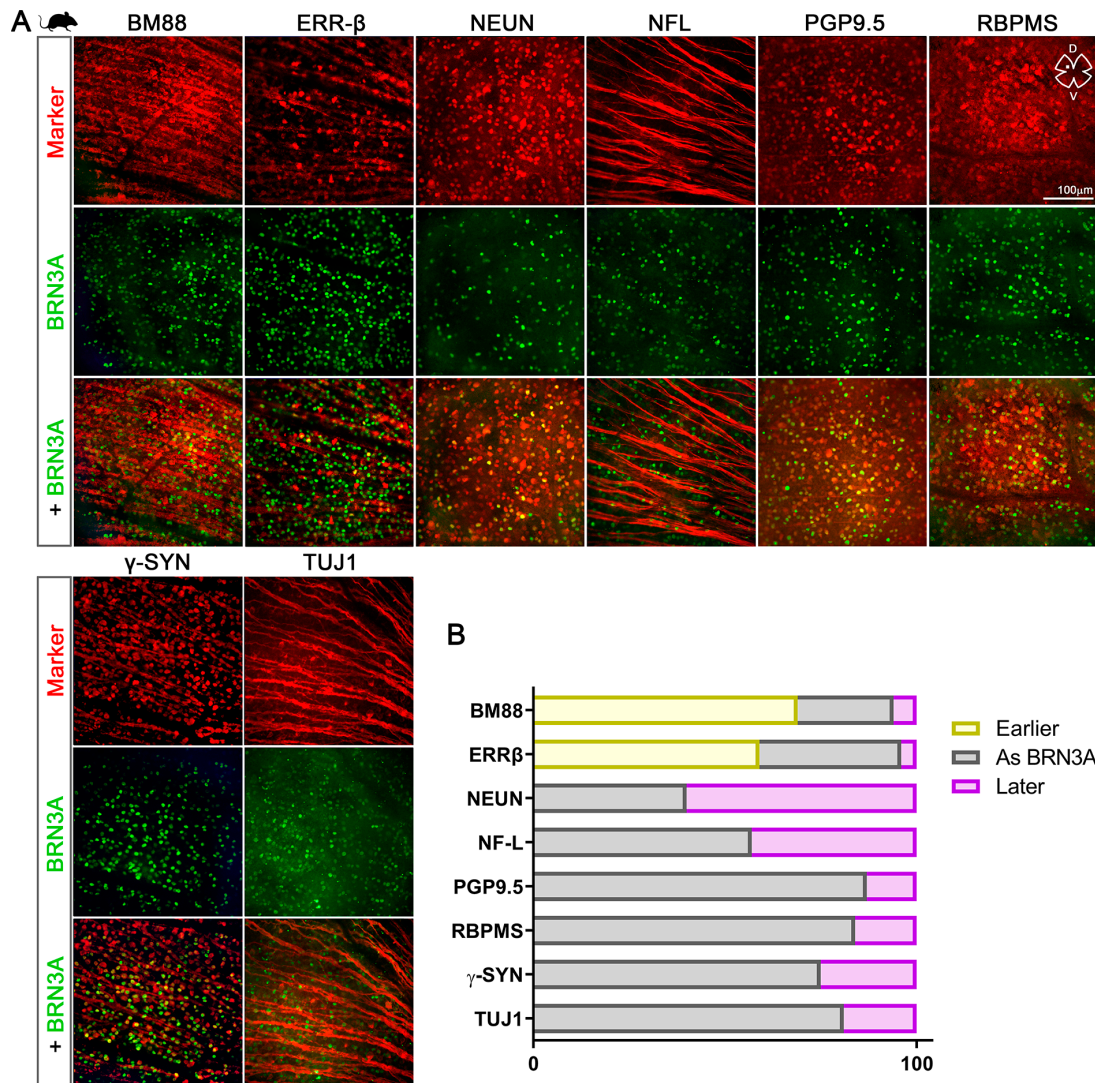


**Figure 5** Marker expression after optic nerve axotomy in mice

A: Double immunodetection of each marker (red) with BRN3A (green) in flat-mounted retinas 5 days after ONC. B: Column graphs in yellow show percentage of RGCs in which the marker is down-regulated earlier than BRN3A, in gray show percentage of RGCs in which BRN3A and marker follow the same regulation, and in purple show percentage of RGCs in which the marker is down-regulated later than BRN3A. 100% is the sum of all quantified cells.

impair visualization of RGC somas in the central retina was verified in cross-sections.  $\gamma$ -SYN expression was studied in mice using a mouse  $\alpha$ - $\gamma$ -SYN antibody, as its specificity has been verified in  $\gamma$ -SYN-deficient animals (Nguyen et al., 2011). In rats and macaques, we used a rabbit anti- $\gamma$ -SYN antibody (Nadal-Nicolás et al., 2015b). Assuming that the antibodies were antigen-specific, as only m- $\alpha$ BRN3A and m- $\alpha$   $\gamma$ -SYN have been validated in knock-out tissue, RGC specificity for all markers was determined (Table 1).

Calculated percentages are shown in Figure 1 and figure legends.

## RESULTS AND DISCUSSION

### Rats

In rats, all markers labeled >90% of traced RGCs (Figure 2A,

B; Table 2). However, both NEUN and PGP.9 detected 38% of cells in the GCL that were not RGCs (Figure 2; gray bars Table 3), thus hindering their use as specific RGC markers. As expected, r- $\alpha$   $\gamma$ -SYN was also detected in non-RGCs (54%).

The most well-defined signals were those of BRN3A, NEUN, and RBPMS, with nuclear or cytoplasmic expression patterns enabling easier quantification. ERR- $\beta$  expression was also cytoplasmic but the signals were not clear. BM88 signals were not well defined and were observed in the somas of RGCs and weakly in their axons. TUJ1, NF-L, and  $\gamma$ -SYN (m), although RGC-specific, displayed an axonal expression, which obscured the RGC somas in the central retina, thus impairing their use for quantification of flat-mounts. Of these markers, axonal staining was the most defined for TUJ1 and NF-L.

BM88, NEUN NF-L, PGP9.5, and  $\gamma$ -SYN (m) were expressed in neurons of the inner nuclear layer (INL)

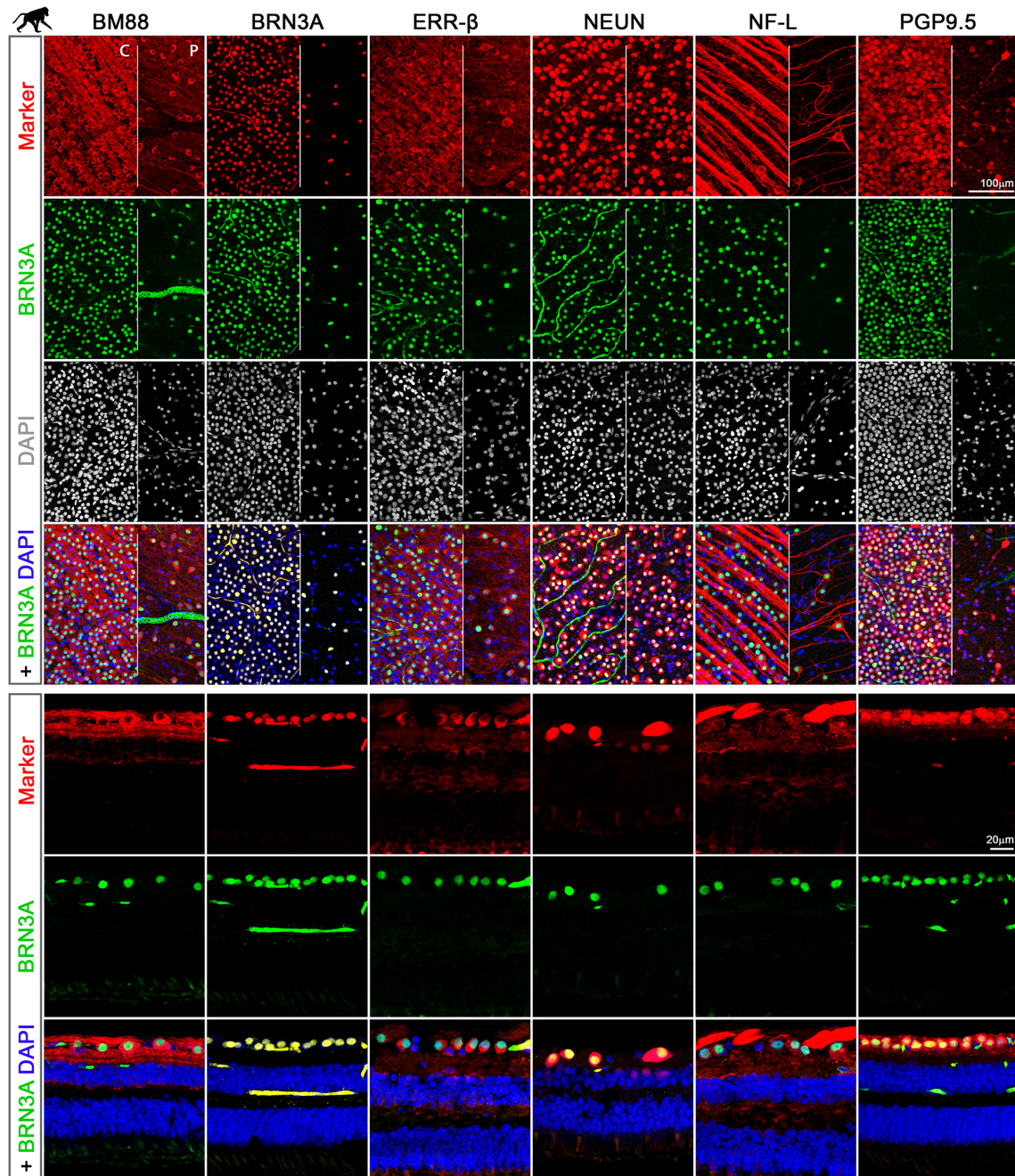


**Figure 6** BM88, BRN3A, ERR- $\beta$ , NEUN NF-L, and PGP9.5 expression in intact rhesus macaque retina

Double immunodetection of each marker (red) and BRN3A (green) in retinal flat-mounts and cross-sections counterstained with DAPI (blue). In flat-mounts, images are shown from central (C) and peripheral (P) retina.

(Figure 2, cross-sections), with ERR- $\beta$ , NF-L, and TUJ1 also expressed in the IPL processes. This is not a problem in the layered retinal structure but may cause artefacts in degenerating retinas (García-Ayuso et al., 2019a).

We next assessed the percentage of RGCs in the GCL by quantifying the number RBPMS-positive or non-positive DAPI<sup>+</sup> nuclei (Figure 2C; Table 4). Data showed that 41% of cells in the GCL (on average) were RGCs, and thus 59% of cells in the GCL were not RGCs, with a higher percentage in the peripheral than in the central retina, consistent with previous

research (Nadal-Nicolás et al., 2015c).

We also detected BRN3A in the same flat-mounts to infer the population of ipRGCs, as ipRGCs are RBPMS<sup>+</sup> and BRN3A<sup>-</sup>. As shown in Figure 2C and Table 4, in rats, the estimated functional subpopulation was 2.4% (Galindo-Romero et al., 2013b; Nadal-Nicolás et al., 2014).

Finally, we investigated the down-regulation of each marker compared to BRN3A (marker of viability, Sánchez-Migallón et al., 2016) in a model of RGC death (Figure 3; Table 5). After ONC, only ERR- $\beta$  and BM88 were down-regulated

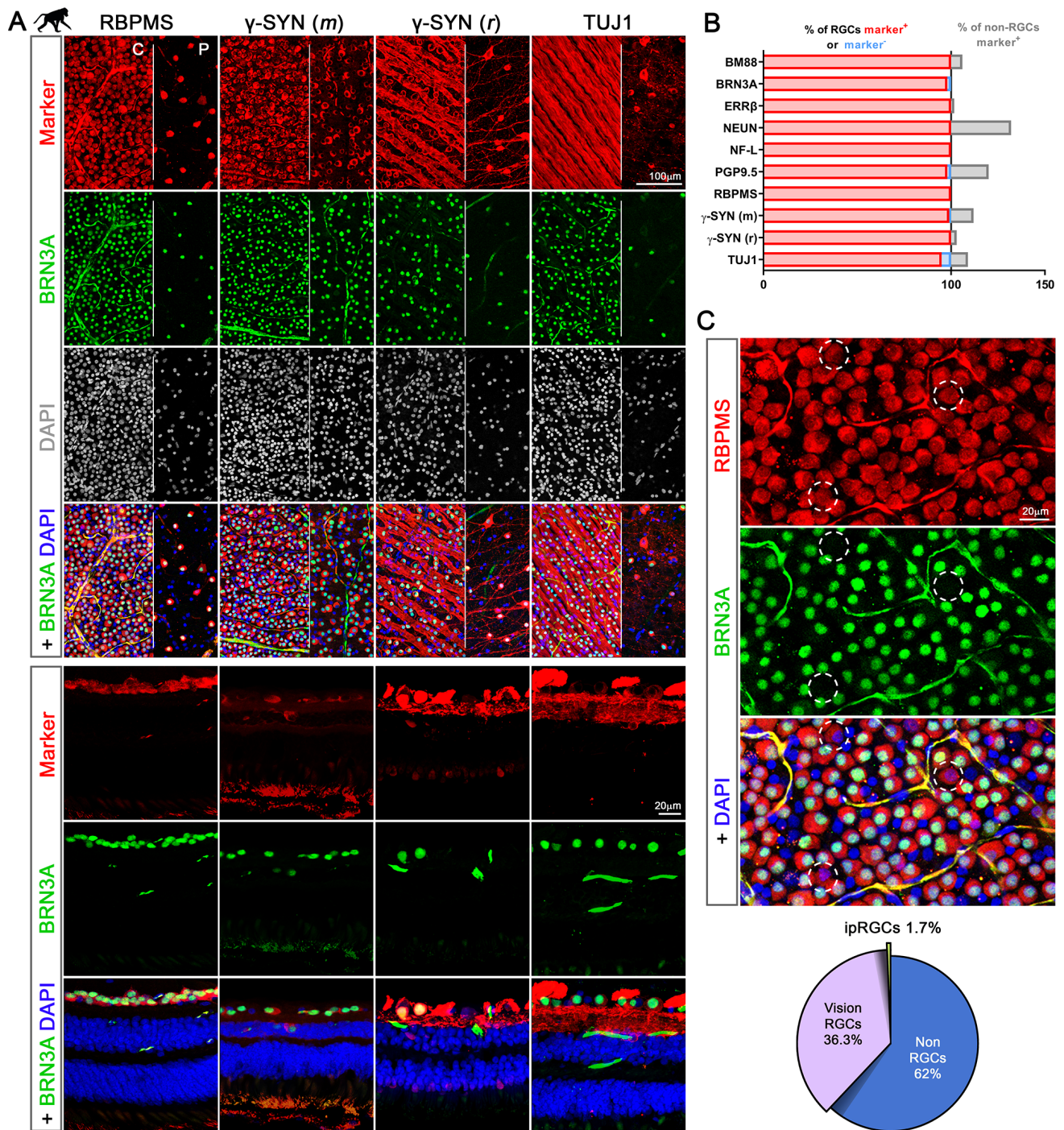


**Figure 7** RBPMS,  $\gamma$ -SYN, and TUJ1 expression in intact rhesus macaque retina

A: Double immunodetection of each marker (red) and BRN3A (green) in retinal flat-mount and resections counterstained with DAPI (blue). In flat-mounts, images are shown from central (C) and peripheral (P) retina.  $\gamma$ -SYN was immunodetected with two different primary antibodies, one raised in mice (*m*) and one in rabbits (*rb*). See text for further explanation. B: Column graphs in red show percentage of RGCs that express each marker (number of BRN3A<sup>+</sup> marker<sup>+</sup> RGCs over total number of BRN3A<sup>+</sup>RGCs), in blue show percentage of RGCs that do not express the marker (number of BRN3A<sup>+</sup> marker<sup>-</sup> RGCs over total number of BRN3A<sup>+</sup>-RGCs), and in gray show percentage of non-RGCs in GCL that express the marker (number of BRN3A<sup>-</sup>marker<sup>+</sup> cells over total number of marker<sup>+</sup> cells). C: Top: Magnifications showing RBPMS and BRN3A immunodetection with DAPI nuclear counterstaining in flat-mounts. Dashed circles mark RBPMS<sup>+</sup> BRN3A<sup>-</sup> RGCs. Bottom: Part of a whole graph showing percentage of RGCs (purple, vision forming; green, ipRGCs) and non-RGCs (blue) in GCL. DAPI<sup>+</sup> RBPMS<sup>+</sup>: RGCs; DAPI<sup>+</sup> RBPMS<sup>-</sup> cells: non-RGCs (of DAPI<sup>+</sup> nuclei); RBPMS<sup>+</sup> BRN3A<sup>-</sup> cells: ipRGCs (of RBPMS<sup>+</sup> cells). Within 38% of RGCs, 1.7% were estimated as ipRGCs.

**Table 1 Primary antibodies and working dilutions**

Antigen	Antibody	Dilution			Cat. number and company
		Mouse	Rat	Macaque	
BM88	r $\alpha$ -BM88	1:50 flat-mounts, 1:200 sections	1:250	1:250	sc-138750, Santa Cruz Biotechnologies, Germany
BRN3A	g $\alpha$ -Brn3a	1:500	1:500	1:500	sc-31984, Santa Cruz Biotechnologies, Germany
BRN3A	m $\alpha$ -Brn3a*	1:300	N/A	N/A	MAB1585, Millipore, Spain
ERR- $\beta$	r $\alpha$ -ERR- $\beta$	1:500	1:200	1:200	E0156 Sigma-Aldrich, Spainab288, 14C8 Abcam, UK
NF-L	r $\alpha$ -NF-L	1:200	1:500	1:500	AB9568, Millipore, Spain
NEUN	m $\alpha$ -NeuN	1:500	1:250	1:250	MAB377, Millipore, Spain
PGP9.5	r $\alpha$ -PGP9.5	1:100	1:500	1:500	ab10404, Abcam, UK
BPMS	r $\alpha$ -BPMS	1:500	1:500	1:500	GTX118619, GeneTex, Spain
$\gamma$ -synuclein	m $\alpha$ - $\gamma$ synuclein*	1:1 000	1:50	1:50	H000006623-M01, Abnova, Spain
$\gamma$ -synuclein	r $\alpha$ - $\gamma$ synuclein	N/A	1:250	1:250	ab55424, Abcam, UK
Tuj1	r $\alpha$ - $\beta$ III Tubulin	1:5 000	1:500	1:500	T-2200, Sigma-Aldrich, Spain

Secondary antibodies were obtained from Molecular Probes (ThermoFisher Scientific., Spain) conjugated with Alexa 488 or Alexa 594. All were used at a 1:500 dilution. m: mouse; r: rabbit; g: goat. \*: Antigen specificity verified in knockout mice. Note, discontinued goat anti BRN3A from Santa Cruz Biotechnology (Germany) was substituted by mouse anti-BRN3A (Millipore, Spain). N/A: Not applicable.

**Table 2 Percentage of RGCs expressing each marker**

Marker	Location	Percentage of traced RGCs marker <sup>+</sup> (%)		Percentage of cells BRN3A <sup>+</sup> marker <sup>+</sup> (%)
		Rat	Mouse	Macaque
BM88	Center	97	56	100
	Periphery	91	43	100
	Mean	94	50	100
BRN3A	Center	98	92	N/A
	Periphery	96	90	N/A
	Mean	97	91	N/A
ERR- $\beta$	Center	100	87	100
	Periphery	100	90	100
	Mean	100	88	100
NEUN	Center	100	100	100
	Periphery	100	100	100
	Mean	100	100	100
NF-L	Center	96	60	100
	Periphery	97	39	100
	Mean	97	50	100
PGP9.5	Center	100	75	97
	Periphery	100	95	99
	Mean	100	85	98
BPMS	Center	100	100	100
	Periphery	100	100	100
	Mean	100	100	100
$\gamma$ -SYN (m)	Center	97	92	100
	Periphery	100	86	98
	Mean	98	89	99
$\gamma$ -SYN (r)	Center	100	N/A	100
	Periphery	100	N/A	100
	Mean	100	N/A	100
TUJ1	Center	100	89	100
	Periphery	100	76	90
	Mean	100	83	95

Percentage of traced RGCs (rats and mice) or Brn3a<sup>+</sup> RGCs (macaques) expressing each marker in center and periphery of retina, and mean expression in whole retina. In rats and macaques,  $\gamma$ -synuclein was immunodetected with two different antibodies (rabbit -r- and mouse -m-, see text for details). N/A: Not applicable.

**Table 3 Marker expression in non-RGCs**

Marker	Location	Percentage of tracer <sup>+</sup> marker <sup>+</sup> cells (%)		Percentage of BRN3A <sup>+</sup> marker <sup>+</sup> cells (%)
		Rat	Mouse	Macaque
BM88	Center	1.9	1	4.8
	Periphery	3.2	1	6.2
	Mean	2.6	1	5.7
BRN3A	Center	1.3	0	N/A
	Periphery	1.7	0	N/A
	Mean	1.5	0	N/A
ERR-β	Center	0	0	2.2
	Periphery	0	0.7	1.3
	Mean	0	0.3	1.7
NEUN	Center	31	11	23
	Periphery	45	15	45
	Mean	38	13	32
NF-L	Center	14	0	0
	Periphery	18	0	0
	Mean	16	0	0
PGP9.5	Center	35	0	7.5
	Periphery	42	0	31
	Mean	38	0	20
RBPMS	Center	1.2	0	2.1
	Periphery	2.2	0	1.3
	Mean	1.7	0	1.7
γ-SYN (m)	Center	1.4	0	18
	Periphery	1.8	0	3.9
	Mean	1.6	0	12
γ-SYN (r)	Center	45	N/A	3.9
	Periphery	63	N/A	2.7
	Mean	54	N/A	3
TUJ1	Center	7	0	9
	Periphery	13	0	9
	Mean	10	0	9

Rat and mouse: Percentage of tracer<sup>+</sup> marker<sup>+</sup> cells in center and periphery of retina, and mean expression in whole retina. Macaque: Percentage of Brn3a<sup>+</sup> marker<sup>+</sup> cells in center and periphery of retina, and mean expression in whole retina. N/A: Not applicable.

**Table 4 Percentage of RGCs and ipRGCs in GCL**

Location	Percentage of RGCs in GCL DAPI <sup>+</sup> RBPMS <sup>+</sup> (%)			Percentage of ipRGCs DAPI <sup>+</sup> BRN3A <sup>+</sup> RBPMS <sup>+</sup> (%)		
	Rat	Mouse	Macaque	Rat	Mouse	Macaque
Center	49	53	60	1.5	8	2.1
Periphery	34	43	21	3.2	7	1.3
Mean	41	49	38	2.4	7.5	1.7

RGCs: Percentage of DAPI<sup>+</sup> nuclei in GCL expressing RBPMS in center and periphery of retina, and mean expression in whole retina. ipRGCs: Percentage of DAPI<sup>+</sup> nuclei in GCL not expressing Brn3a but expressing RBPMS in center and periphery of retina, and mean expression in whole retina.

earlier than BRN3A, with ERR-β showing the most significant down-regulation as it lost expression in all RGCs. BM88 was expressed as BRN3A in 66% of RGCs and disappeared later than BRN3A in 20% of RGCs. The remaining markers behaved as BRN3A or showed later down-regulation: γ-SYN (m), TUJ1, and NF-L were co-expressed with BRN3A in 77%, 77%, and 65% of RGCs, respectively, while RBPMS expression was very similar to that of BRN3A, with a delay in 13% of RGCs. NEUN and PGP.9 showed a higher percentage

of late down-regulation than other markers (51% and 56% respectively), consistent with the expression of these markers in non-RGCs in the GCL, possibly displaced amacrine cells, which are the only other neurons in this layer. γ-SYN (r) down-regulation showed a delay (68%), as displaced amacrine cells were also detected by the antibody.

#### Mice

In mice, 50% of traced RGCs were labeled by BM88 and

**Table 5 Marker expression after optic nerve crush in rodents**

Marker	Location	Rat			Mouse		
		% BRN3A <sup>+</sup> marker <sup>+</sup>	% BRN3A <sup>+</sup> marker <sup>-</sup>	% BRN3A <sup>-</sup> marker <sup>+</sup>	% BRN3A <sup>+</sup> marker <sup>+</sup>	% BRN3A <sup>+</sup> marker <sup>-</sup>	% BRN3A <sup>-</sup> marker <sup>+</sup>
BM88	Center	76	6	18	28	65	7
	Periphery	64	13	22	22	73	5
	Mean	70	10	20	25	69	6
ERR-β	Center	0	100	0	39	55	7
	Periphery	0	100	0	35	63	2
	Mean	0	100	0	37	59	4
NEUN	Center	56	0	44	41	0	59
	Periphery	43	0	57	40	0	61
	Mean	49	0	51	40	0	60
NFL	Center	66	0	34	53	0	47
	Periphery	65	0	35	61	0	39
	Mean	65	0	35	57	0	43
PGP9.5	Center	50	0	50	84	0	16
	Periphery	37	0	63	90	0	10
	Mean	44	0	56	87	0	13
RBPMS	Center	91	0	9	81	0	20
	Periphery	83	0	16	87	0	13
	Mean	87	0	13	84	0	16
γ-SYN (m)	Center	83	0	17	75	0	25
	Periphery	73	0	26	75	0	25
	Mean	78	0	22	75	0	25
γ-SYN (r)	Center	40	0	59	N/A	N/A	N/A
	Periphery	24	0	76	N/A	N/A	N/A
	Mean	32	0	68	N/A	N/A	N/A
TUJ1	Center	84	0	16	77	0	23
	Periphery	71	0	29	86	0	15
	Mean	77	0	23	81	0	19

Percentage of cells quantified 5 days after ONC expressing Brn3a and marker, expressing Brn3a but not marker, or expressing marker but not Brn3a (i.e., expression of the marker parallels expression of the gold standard to analyze RGC death (Brn3a), its expression is lost earlier than that of Brn3a, or its expression is maintained longer than that of Brn3a, respectively). Data are from the center and periphery of the retina, and mean expression across the whole retina. Co-localization analysis was performed in flat mounts. In rats, γ-synuclein was immunodetected with two different antibodies (rabbit -r- and mouse -m-, see text for more details). N/A: Not applicable

NF-L, >80% were labeled by ERR-β, PGP9.5, γ-SYN, and TUJ1, >90% were labeled by BRN3A, and 100% were labeled by RBPMS (Figure 4; Table 2).

Similar to rats, the best somatic/nuclear marker signals were BRN3A, NEUN, and RBPMS. In mice, only NEUN labeled non-RGCs in the GCL (10% of cells, Figure 4; Table 3). Staining of other retinal layers was only observed for BM88, ERR-β, and TUJ1, which labeled the IPL, and for NEUN, which was expressed in neuronal nuclei in the INL. As in rats, axonal markers impaired RGC soma visualization, and clearer axonal labeling was observed with NF-L and TUJ1.

Mice exhibited a slightly higher percentage of RGCs in the GCL than rats (49% in mice vs. 41% in rats), with an estimated percentage of ipRGCs of 7.5%, (Figure 4; Table 4), much higher than that of the immunodetected m<sup>+</sup> RGCs (2.0%–2.5%) (Valiente-Soriano et al., 2014) and consistent with the believed number of ipRGCs (Chen et al., 2021).

After ONC, BM88 and ERR-β were down-regulated earlier than BRN3A, although ERR-β down-regulation was not as severe as that in rats and its expression followed BRN3A in 37% of RGCs. NEUN, NF-L, and γ-SYN showed a delayed

down-regulation compared to BRN3A in 60%, 43%, and 25% of RGCs, respectively. The higher percentage of NEUN+ BRN3A- cells is consistent with the fact that this protein is expressed in non-RGCs, as observed in rats. More than 80% of RGCs showed the same regulation for BRN3A and RBPMS, BRN3A and TUJ1, and BRN3A and PGP9.5 (Figure 5; Table 5).

### Macaques

Analyses differed in this species as neither retrograde tracing of RGCs nor ONC were feasible. In the macaque retina, more than 95% of RGCs showed co-expression of each marker and BRN3A (Figures 6, 7; Table 2). In addition, NEUN, PGP9.5, γ-SYN (m), and TUJ1 were expressed in 32%, 20%, 12%, and 9% of BRN3A-negative cells (Figures 6, 7; Table 3). The rabbit anti-γ-SYN antibody was more RGC-specific in the macaque retina than in the rat retina, with only 3% of BRN3A- cells detected with this antibody. BM88, ERR-β, NF-L, γ-SYN (r), and TUJ1 signals were found in the IPL, as also observed in rodents. Finally, γ-SYN (r) expression was observed in somas located in the INL.

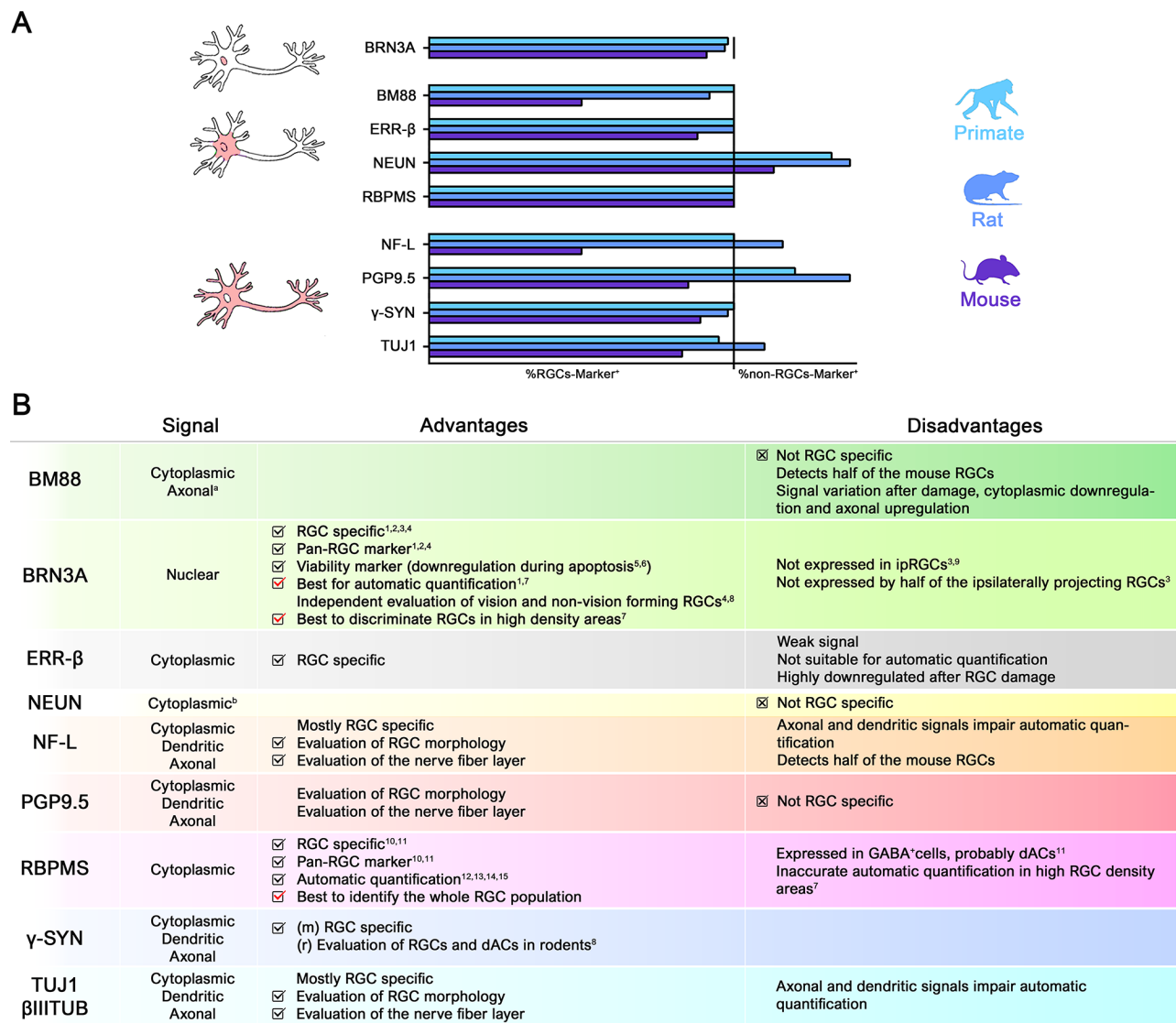


**Figure 8 Review summary**

A: Percentage of RGCs and non-RGCs expressing each marker in each species. Drawings of neurons in light red indicate expression pattern of different markers in rats, mice, and macaques: nuclear, cytoplasmic, and cytoplasmic/axonal/dendritic. B: Summary of advantages and disadvantages of each marker. <sup>1</sup>: Nadal-Nicolas et al., 2009; <sup>2</sup>: Galindo-Romero et al., 2011; <sup>3</sup>: Nadal-Nicolas et al., 2012; <sup>4</sup>: Nadal-Nicolas et al., 2014; <sup>5</sup>: Sanchez-Migallon et al., 2016; <sup>6</sup>: Nadal-Nicolas et al., 2017; <sup>7</sup>: Xiao et al., 2021; <sup>8</sup>: Nadal-Nicolas et al., 2015b; <sup>9</sup>: Cheng et al., 2015; <sup>10</sup>: Kwong et al., 2010; <sup>11</sup>: Rodriguez et al., 2014; <sup>12</sup>: Dordea et al., 2016; <sup>13</sup>: Guymer et al., 2020; <sup>14</sup>: Masin et al., 2021; <sup>15</sup>: Zhang et al., 2022. <sup>a</sup>: BM88 signal is predominantly cytoplasmic, although axons are faintly detected. BM88 axonal expression in macaques is stronger than in rodents. <sup>b</sup>: NEUN expression is perinuclear/cytoplasmic in RGCs. m: mouse anti-γ-SYN; r: rabbit anti-γ-SYN.

Interestingly, while the percentage of non-RGCs in the GCL was 10%–15% higher in the center than in the periphery in rats and mice, this difference was close to three-fold higher in the macaques. In addition, the percentage of RGCs in the GCL was smaller in macaques than in rodents (38% in macaques vs. 41%–49% in rodents) and the inferred subpopulation of ipRGCs was close to 2% (Figure 7; Table 4).

### CONCLUDING REMARKS

This is the first work to systematically address the expression patterns of nine proteins commonly used to identify RGCs in three different species. Mice and rats are widely used in

preclinical studies, while research on non-human primates is of great interest from a developmental, neuroanatomical, and physiological point of view given their highly similarity to humans, which facilitates translation (Nadal-Nicolás et al., 2022). However, due to high costs and ethical considerations, monkeys are not used as often as rodents, although this is changing in the fields of stem cell therapy and induced pluripotent stem cells (Lingam et al., 2021; Liu et al., 2021; Lopez et al., 2022).

Nuclear and cytoplasmic markers are more suitable for quantification of RGCs, with BRN3A and RBPMS being the most specific in the three species (Figure 8). Thus, these two



markers are the current markers of choice. Their main difference is that BRN3A is expressed in vision-forming RGCs (91% to 98% of RGCs, depending on the species) but not in ipRGCs (2% to 7.5% of RGCs (Chen et al., 2011; Nadal-Nicolás et al., 2012)). This is an advantage when studying functional populations separately. Methodologically, nuclear BRN3A signals do not overlap with RGC somas, thus enabling easier manual and automated quantification (Galindo-Romero et al., 2011; Geeraerts et al., 2016; Masin et al., 2021; Miesfeld et al., 2020; Nadal-Nicolás et al., 2009; Sánchez-Migallón et al., 2011). Automatic algorithms of RBPMS are reliable and efficient in mouse retinas (Dordea et al., 2016; Guymier et al., 2020; Masin et al., 2021; Zhang et al., 2022), but in other species, e.g., ground squirrels, high-density RGC areas impair soma discrimination and accurate quantification (Xiao et al., 2021).

The delay between RBPMS and BRN3A may be due to several reasons. First, RBPMS is also expressed in ipRGCs, which are more resistant to axotomy than vision-forming RGCs (Nadal-Nicolás et al., 2015a; Sánchez-Migallón et al., 2018a), and second, BRN3A is a marker of viability and is down-regulated in death-committed RGCs, independent of microglial clearance. Nevertheless, this delay is small, and while BRN3A<sup>+</sup> RGC death will be observed slightly earlier and may be more pronounced, it is not a problem if all retinas within an experimental setting are analyzed with the same marker.

NEUN expression in RGCs was cytoplasmic in the three species. In rodents, but not in macaques, NEUN was also expressed in the INL with nuclear signals. NEUN is expressed in all RGCs, and its cytoplasmic signal is advantageous for quantification. However, a considerable proportion of non-RGCs also express this transcription factor in the GCL, disqualifying it as a specific RGC marker.

The other two cytoplasmic markers also exhibit drawbacks. Here, ERR- $\beta$  recognized >85% of RGCs in the three species but with relatively poor signals. In addition, in rats and in a good proportion of RGCs in mice, its regulation did not follow actual RGC death. Therefore, this marker should not be used in survival and neuroprotection studies. In rats and macaques, but not in mice, BM88 labeled most RGCs but again with relatively poorly defined signals.

Axonal/somatic markers are useful for studying axonal degeneration but not for quantifying RGCs. Of these markers,  $\gamma$ -SYN was the most specific and was expressed by the majority of RGCs in all three species. In humans and mice,  $\gamma$ -SYN is expressed by astrocytes in the optic nerve only under disease conditions, and thus may not be a good axonal marker under pathological situations (Liu et al., 2020; Nguyen et al., 2011). We also found that PGP9.5 was labeled in 85% of RGCs in mice and in all RGCs in macaques and rats, although it was also expressed in non-RGCs in the latter two species. TUJ1 and NF-L showed very well-defined signals, but NF-L was only detected in 50% of RGCs in mice and both markers labeled non-RGCs in rats.

Some markers are also expressed in other retinal layers, which is not a problem per se. Those labeling the IPL can also be used to analyze cross-sections to determine the fate of RGC dendrites after lesion.

We also deduced the proportion of ipRGCs, ranging from 1.7% (macaques) to 7.5% (mice). Furthermore, in all three species, RGC density was lower in the periphery and the percentage of non-RGCs in the GCL exceeded 50%.

In summary, when analyzing RGCs, the choice of marker will depend on the goals of each study. However, specificity is essential to obtain reliable results (Figure 8B). RBPMS is best for examining the entire RGC population, although it may include a small proportion of GABA<sup>+</sup> dACs (Rodríguez et al., 2014). BRN3A allows assessment of areas of high RGC density (Xiao et al., 2021), as well as separate analysis of image-forming and non-image-forming RGCs.

## COMPETING INTERESTS

The authors declare that they have no competing interests.

## AUTHORS' CONTRIBUTIONS

F.M.N.N., C.G.R., and M.A.B. conceived and designed the study, analyzed the data, and prepared the figures. F.L.R. analyzed the data and prepared the figures. N.M.A., L.W., N.S., and M.V.S. participated in manuscript revision. M.A.B. wrote the first manuscript draft. L.W., M.V.S., and M.A.B. funded the study. All authors read and approved the final version of the manuscript.

## ACKNOWLEDGMENTS

We would like to thank Dr. Lauren Brinster (Diagnostic and Research Services Branch, NIH), Dr. Mark A. Eldridge (National Institute of Mental Health, NIH), and Dr. Julie Mattison and Dr. Kielee Jennings (Non-Human Primate Core of the National Institute on Aging, NIH) for providing post-mortem monkey specimens.

## REFERENCES

- Álvarez-Hernán G, Hernández-Núñez I, Rico-Leo EM, Marzal A, De Mera-Rodríguez JA, Rodríguez-León J, et al. 2020. Retinal differentiation in an altricial bird species, *Taeniopygia guttata*: an immunohistochemical study. *Experimental Eye Research*, **190**: 107869.
- Ávila-García M, García-Sánchez G, Lira-Romero E, Moreno-Mendoza N. 2012. Characterization of progenitor cells during canine retinal development. *Stem Cells International*, **2012**: 675805.
- Avilés-Trigueros M, Sauvé Y, Lund RD, Vidal-Sanz M. 2000. Selective innervation of retinorecipient brainstem nuclei by retinal ganglion cell axons regenerating through peripheral nerve grafts in adult rats. *The Journal of Neuroscience*, **20**(1): 361–374.
- Badea TC, Nathans J. 2011. Morphologies of mouse retinal ganglion cells expressing transcription factors BRN3A, Brn3b, and Brn3c: analysis of wild type and mutant cells using genetically-directed sparse labeling. *Vision Research*, **51**(2): 269–279.
- Baden T, Berens P, Franke K, Rosón MR, Bethge M, Euler T. 2016. The functional diversity of retinal ganglion cells in the mouse. *Nature*, **529**(7586): 345–350.
- Bae JA, Mu S, Kim JS, Turner NL, Tartavull I, Kemnitz N, et al. 2018. Digital museum of retinal ganglion cells with dense anatomy and physiology. *Cell*, **173**(5): 1293–1306.e19.
- Barnstable CJ, Dräger UC. 1984. Thy-1 antigen: a ganglion cell specific

- marker in rodent retina. *Neuroscience*, **11**(4): 847–855.
- Berg DJ, Kartheiser K, Leyrer M, Saali A, Berson DM. 2019. Transcriptomic signatures of postnatal and adult intrinsically photosensitive ganglion cells. *eNeuro*, **6**(4): ENEURO.0022–19.2019.
- Black MM, Lasek RJ. 1980. Slow components of axonal transport: two cytoskeletal networks. *The Journal of Cell Biology*, **86**(2): 616–623.
- Bollaerts I, Veys L, Geeraerts E, Andries L, De Groef L, Buyens T, et al. 2018. Complementary research models and methods to study axonal regeneration in the vertebrate retinofugal system. *Brain Structure and Function*, **223**(2): 545–567.
- Bouskila J, Micaelo-Fernandes C, Palmour RM, Bouchard JF, Ptito M. 2020. Transient receptor potential vanilloid type 1 is expressed in the horizontal pathway of the vervet monkey retina. *Scientific Reports*, **10**(1): 12116.
- Buckingham BP, Inman DM, Lambert W, Oglesby E, Calkins DJ, Steele MR, et al. 2008. Progressive ganglion cell degeneration precedes neuronal loss in a mouse model of glaucoma. *The Journal of Neuroscience*, **28**(11): 2735–2744.
- Budram-Mahadeo V, Morris PJ, Latchman DS. 2002. The Brn-3a transcription factor inhibits the pro-apoptotic effect of p53 and enhances cell cycle arrest by differentially regulating the activity of the p53 target genes encoding Bax and p21<sup>CIP1/Waf1</sup>. *Oncogene*, **21**(39): 6123–6131.
- Chen CK, Kiyama T, Weber N, Whitaker CM, Pan P, Badea TC, et al. 2021. Characterization of Tbr2-expressing retinal ganglion cells. *The Journal of Comparative Neurology*, **529**(15): 3513–3532.
- Chen SK, Badea TC, Hattar S. 2011. Photoentrainment and pupillary light reflex are mediated by distinct populations of ipRGCs. *Nature*, **476**(7358): 92–95.
- Chidlow G, Casson R, Sobrado-Calvo P, Vidal-Sanz M, Osborne NN. 2005. Measurement of retinal injury in the rat after optic nerve transection: an RT-PCR study. *Molecular Vision*, **11**: 387–396.
- Chidlow G, Osborne NN. 2003. Rat retinal ganglion cell loss caused by kainate, NMDA and ischemia correlates with a reduction in mRNA and protein of Thy-1 and neurofilament light. *Brain Research*, **963**(1–2): 298–306.
- Corral-Domenge C, De La Villa P, Mansilla A, Germain F. 2022. Tools and biomarkers for the study of retinal ganglion cell degeneration. *International Journal of Molecular Sciences*, **23**(8): 4287.
- Cuenca N, De La Villa P. 2021. La Retina de los Vertebrados. Consejo Superior de Investigaciones Científicas.
- Dabin I, Barnstable CJ. 1995. Rat retinal Müller cells express Thy-1 following neuronal cell death. *Glia*, **14**(1): 23–32.
- Darlington PJ, Goldman JS, Cui QL, Antel JP, Kennedy TE. 2008. Widespread immunoreactivity for neuronal nuclei in cultured human and rodent astrocytes. *Journal of Neurochemistry*, **104**(5): 1201–1209.
- Day INM. 1992. Enolases and PGP9.5 as tissue-specific markers. *Biochemical Society Transactions*, **20**(3): 637–642.
- De Lara MJP, Santano C, Guzmán-Aránguez A, Valiente-Soriano FJ, Avilés-Trigueros M, Vidal-Sanz M, et al. 2014. Assessment of inner retina dysfunction and progressive ganglion cell loss in a mouse model of glaucoma. *Experimental Eye Research*, **122**: 40–49.
- Dibas A, Yang MH, He SQ, Bobich J, Yorio T. 2008. Changes in ocular aquaporin-4 (AQP4) expression following retinal injury. *Molecular Vision*, **14**: 1770–1783.
- Dordea AC, Bray MA, Allen K, Logan DJ, Fei F, Malhotra R, et al. 2016. An open-source computational tool to automatically quantify immunolabeled retinal ganglion cells. *Experimental Eye Research*, **147**: 50–56.
- Dräger UC, Hofbauer A. 1984. Antibodies to heavy neurofilament subunit detect a subpopulation of damaged ganglion cells in retina. *Nature*, **309**(5969): 624–626.
- Ecker JL, Dumitrescu ON, Wong KY, Alam NM, Chen SK, LeGates T, et al. 2010. Melanopsin-expressing retinal ganglion-cell photoreceptors: cellular diversity and role in pattern vision. *Neuron*, **67**(1): 49–60.
- Esquivia G, Avivi A, Hannibal J. 2016. Non-image forming light detection by melanopsin, rhodopsin, and long-middlewave (L/W) cone opsin in the subterranean blind mole rat, *Spalax ehrenbergi*: immunohistochemical characterization, distribution, and connectivity. *Frontiers in Neuroanatomy*, **10**: 61.
- Esteve-Rudd J, Campello L, Herrero MT, Cuenca N, Martín-Nieto J. 2010. Expression in the mammalian retina of parkin and UCH-L1, two components of the ubiquitin-proteasome system. *Brain Research*, **1352**: 70–82.
- Farooqui-Kabir SR, Budhram-Mahadeo V, Lewis H, Latchman DS, Marber MS, Heads RJ. 2004. Regulation of Hsp27 expression and cell survival by the POU transcription factor Brn3a. *Cell Death & Differentiation*, **11**(11): 1242–1244.
- Feng L, Zhao Y, Yoshida M, Chen H, Yang JF, Kim TS, et al. 2013. Sustained ocular hypertension induces dendritic degeneration of mouse retinal ganglion cells that depends on cell type and location. *Investigative Ophthalmology & Visual Science*, **54**(2): 1106–1117.
- Gábel R, Straznicky C. 1992. Immunocytochemical localization of parvalbumin- and neurofilament triplet protein immunoreactivity in the cat retina: colocalization in a subpopulation of All amacrine cells. *Brain Research*, **595**(1): 133–136.
- Galindo-Romero C, Avilés-Trigueros M, Jiménez-López M, Valiente-Soriano FJ, Salinas-Navarro M, Nadal-Nicolás F, et al. 2011. Axotomy-induced retinal ganglion cell death in adult mice: quantitative and topographic time course analyses. *Experimental Eye Research*, **92**(5): 377–387.
- Galindo-Romero C, Harun-Or-Rashid M, Jiménez-López M, Vidal-Sanz M, Agudo-Barriuso M, Hallböök F. 2016. Neuroprotection by  $\alpha$ 2-adrenergic receptor stimulation after excitotoxic retinal injury: a study of the total population of retinal ganglion cells and their distribution in the chicken retina. *PLoS One*, **11**(9): e0161862.
- Galindo-Romero C, Jiménez-López M, García-Ayuso D, Salinas-Navarro M, Nadal-Nicolás FM, Agudo-Barriuso M, et al. 2013a. Number and spatial distribution of intrinsically photosensitive retinal ganglion cells in the adult albino rat. *Experimental Eye Research*, **108**: 84–93.
- Galindo-Romero C, Valiente-Soriano FJ, Jiménez-López M, García-Ayuso D, Villegas-Pérez MP, Vidal-Sanz M, et al. 2013b. Effect of brain-derived neurotrophic factor on mouse axotomized retinal ganglion cells and phagocytic microglia. *Investigative Ophthalmology & Visual Science*, **54**(2): 974–985.
- Gallego-Ortega A, Norte-Muñoz M, De Imperial-Ollero JAM, Bernal-Garro JM, Valiente-Soriano FJ, De La Villa P, et al. 2020. Functional and morphological alterations in a glaucoma model of acute ocular hypertension. *Progress in Brain Research*, **256**(1): 1–29.
- García-Ayuso D, Di Pierdomenico J, Valiente-Soriano FJ, Martínez-Vacas A, Agudo-Barriuso M, Vidal-Sanz M, et al. 2019a.  $\beta$ -alanine supplementation induces taurine depletion and causes alterations of the retinal nerve fiber layer and axonal transport by retinal ganglion cells. *Experimental Eye Research*, **188**: 107781.
- García-Ayuso D, Di Pierdomenico J, Vidal-Sanz M, Villegas-Pérez MP.

- 2019b. Retinal ganglion cell death as a late remodeling effect of photoreceptor degeneration. *International Journal of Molecular Sciences*, **20**(18): 4649.
- Geeraerts E, Dekeyster E, Gaublomme D, Salinas-Navarro M, De Groef L, Moons L. 2016. A freely available semi-automated method for quantifying retinal ganglion cells in entire retinal flatmounts. *Experimental Eye Research*, **147**: 105–113.
- Gerber WV, Yatskievych TA, Antin PB, Correia KM, Conlon RA, Krieg PA. 1999. The RNA-binding protein gene, *hermes*, is expressed at high levels in the developing heart. *Mechanisms of Development*, **80**(1): 77–86.
- Ghinia MG, Novelli E, Sajgo S, Badea TC, Strettoi E. 2019. BRN3A and Brn3b knockout mice display unvaried retinal fine structure despite major morphological and numerical alterations of ganglion cells. *The Journal of Comparative Neurology*, **527**(1): 187–211.
- Gioli RA, Towns LC. 1980. A review of axon collateralization in the mammalian visual system. *Brain, Behavior and Evolution*, **17**(5): 364–390.
- Gong B, Leznik E. 2007. The role of ubiquitin C-terminal hydrolase L1 in neurodegenerative disorders. *Drug News & Perspectives*, **20**(6): 365–370.
- Gordon KJ, Blobel GC. 2008. Role of transforming growth factor- $\beta$  superfamily signaling pathways in human disease. *Biochimica et Biophysica Acta (BBA) - Molecular Basis of Disease*, **1782**(4): 197–228.
- Grillo SL, Stella SL Jr. 2018. Melanopsin retinal ganglion cells are not labeled in Thy-1 YFP-16 transgenic mice. *Neuroreport*, **29**(2): 118–122.
- Gusel'nikova VV, Korzhhevskiy DE. 2015. NEUN as a neuronal nuclear antigen and neuron differentiation marker. *Acta Naturae*, **7**(2): 42–47.
- Guymier C, Damp L, Chidlow G, Wood J, Tang YF, Casson R. 2020. Software for quantifying and batch processing images of Brn3a and RBPMS immunolabeled retinal ganglion cells in retinal wholemounts. *Translational Vision Science & Technology*, **9**(6): 28.
- Harada T, Harada C, Wang YL, Osaka H, Amanai K, Tanaka K, et al. 2004. Role of ubiquitin carboxy terminal hydrolase-L1 in neural cell apoptosis induced by ischemic retinal injury *in vivo*. *The American Journal of Pathology*, **164**(1): 59–64.
- Hattar S, Kumar M, Park A, Tong P, Tung J, Yau KW, et al. 2006. Central projections of melanopsin-expressing retinal ganglion cells in the mouse. *The Journal of Comparative Neurology*, **497**(3): 326–349.
- Hayworth CR, Rojas JC, Gonzalez-Lima F. 2008. Transgenic mice expressing cyan fluorescent protein as a reporter strain to detect the effects of rotenone toxicity on retinal ganglion cells. *Journal of Toxicology and Environmental Health, Part A*, **71**(24): 1582–1592.
- Hirata M, Shearer TR, Azuma M. 2015. Hypoxia activates calpains in the nerve fiber layer of monkey retinal explants. *Investigative Ophthalmology & Visual Science*, **56**(10): 6049–6057.
- Hirsch N, Harris WA. 1997. Xenopus Brn-3.0, a POU-domain gene expressed in the developing retina and tectum. Not regulated by innervation. *Investigative Ophthalmology & Visual Science*, **38**(5): 960–969.
- Hoffman PN, Lasek RJ. 1975. The slow component of axonal transport. Identification of major structural polypeptides of the axon and their generality among mammalian neurons. *The Journal of Cell Biology*, **66**(2): 351–366.
- Hörnberg H, Horck FWV, Maurus D, Zwart M, Svoboda H, Harris WA, et al. 2013. RNA-binding protein Hermes/RBPMS inversely affects synapse density and axon arbor formation in retinal ganglion cells *in vivo*. *The Journal of Neuroscience*, **33**(25): 10384–10395.
- Huang EJ, Liu W, Fritzsche B, Bianchi LM, Reichardt LF, Xiang MQ. 2001. BRN3A is a transcriptional regulator of soma size, target field innervation and axon pathfinding of inner ear sensory neurons. *Development*, **128**(13): 2421–2432.
- Huang W, Fileta J, Guo Y, Grosskreutz CL. 2006. Downregulation of Thy1 in retinal ganglion cells in experimental glaucoma. *Current Eye Research*, **31**(3): 265–271.
- Hudson CD, Morris PJ, Latchman DS, Budhram-Mahadeo VS. 2016. Brn-3a transcription factor blocks p53-mediated activation of proapoptotic target genes Noxa and Bax *in vitro* and *in vivo* to determine cell fate. *The Journal of Biological Chemistry*, **291**(30): 15909.
- laboni DSM, Farrell SR, Chauhan BC. 2020. Morphological multivariate cluster analysis of murine retinal ganglion cells selectively expressing yellow fluorescent protein. *Experimental Eye Research*, **196**: 108044.
- Ikeda T, Nakamura K, Oku H, Horie T, Kida T, Takai S. 2019. Immunohistological study of monkey foveal retina. *Scientific Reports*, **9**(1): 5258.
- Jain V, Ravindran E, Dhingra NK. 2012. Differential expression of Brn3 transcription factors in intrinsically photosensitive retinal ganglion cells in mouse. *The Journal of Comparative Neurology*, **520**(4): 742–755.
- Jara JH, Frank DD, Özdinler PH. 2013. Could dysregulation of UPS be a common underlying mechanism for cancer and neurodegeneration? Lessons from UCHL1. *Cell Biochemistry and Biophysics*, **67**(1): 45–53.
- Jeon CJ, Strettoi E, Masland RH. 1998. The major cell populations of the mouse retina. *The Journal of Neuroscience*, **18**(21): 8936–8946.
- Johansson UE, Eftekhari S, Warfvinge K. 2010. A battery of cell- and structure-specific markers for the adult porcine retina. *The Journal of Histochemistry & Cytochemistry*, **58**(4): 377–389.
- Jung C, Yabe JT, Shea TB. 2000. C-terminal phosphorylation of the high molecular weight neurofilament subunit correlates with decreased neurofilament axonal transport velocity. *Brain Research*, **856**(1–2): 12–19.
- Kalesnykas G, Oglesby EN, Zack DJ, Cone FE, Steinhart MR, Tian J, et al. 2012. Retinal ganglion cell morphology after optic nerve crush and experimental glaucoma. *Investigative Ophthalmology & Visual Science*, **53**(7): 3847–3857.
- Karnas D, Mordel J, Bonnet D, Pévet P, Hicks D, Meissl H. 2013. Heterogeneity of intrinsically photosensitive retinal ganglion cells in the mouse revealed by molecular phenotyping. *The Journal of Comparative Neurology*, **521**(4): 912–932.
- Katsimpardi L, Gaitanou M, Malnou CE, Lledo PM, Charneau P, Matsas R, et al. 2008. BM88/Cend1 expression levels are critical for proliferation and differentiation of subventricular zone-derived neural precursor cells. *Stem Cells*, **26**(7): 1796–1807.
- Kay JN, De La Huerta I, Kim IJ, Zhang YF, Yamagata M, Chu MW, et al. 2011. Retinal ganglion cells with distinct directional preferences differ in molecular identity, structure, and central projections. *The Journal of Neuroscience*, **31**(21): 7753–7762.
- Kim CY, Kuehn MH, Clark AF, Kwon YH. 2006. Gene expression profile of the adult human retinal ganglion cell layer. *Molecular Vision*, **12**: 1640–1648.
- Kim KK, Adelstein RS, Kawamoto S. 2009. Identification of neuronal nuclei (NeuN) as Fox-3, a new member of the Fox-1 gene family of splicing factors. *The Journal of Biological Chemistry*, **284**(45): 31052–31061.
- Kim KK, Nam J, Mukoyama YS, Kawamoto S. 2013. Rbfox3-regulated alternative splicing of Numb promotes neuronal differentiation during development. *The Journal of Cell Biology*, **200**(4): 443–458.
- Kim US, Mahroo OA, Mollon JD, Yu-Wai-Man P. 2021. Retinal ganglion cells-diversity of cell types and clinical relevance. *Frontiers in Neurology*,

12: 661938.

- Kong WC, Cho EYP. 1999. Antibodies against neurofilament subunits label retinal ganglion cells but not displaced amacrine cells of hamsters. *Life Sciences*, **64**(19): 1773–1778.
- Koutmani Y, Hurel C, Patsavoudi E, Hack M, Gotz M, Thomaidou D, et al. 2004. BM88 is an early marker of proliferating precursor cells that will differentiate into the neuronal lineage. *The European Journal of Neuroscience*, **20**(10): 2509–2523.
- Kunst S, Wolloscheck T, Grether M, Trunsch P, Wolfrum U, Spessert R. 2015. Photoreceptor cells display a daily rhythm in the orphan receptor Esrr $\beta$ . *Molecular Vision*, **21**: 173–184.
- Kwong JMK, Caprioli J, Piri N. 2010. RNA binding protein with multiple splicing: a new marker for retinal ganglion cells. *Investigative Ophthalmology & Visual Science*, **51**(2): 1052–1058.
- Kwong JMK, Quan A, Kyung H, Piri N, Caprioli J. 2011. Quantitative analysis of retinal ganglion cell survival with RBPMS immunolabeling in animal models of optic neuropathies. *Investigative Ophthalmology & Visual Science*, **52**(13): 9694–9702.
- Lafuente MP, Villegas-Pérez MP, Sellés-Navarro I, Mayor-Torroglosa S, De Imperial JM, Vidal-Sanz M. 2002. Retinal ganglion cell death after acute retinal ischemia is an ongoing process whose severity and duration depends on the duration of the insult. *Neuroscience*, **109**(1): 157–168.
- Lansbury PT Jr. 2006. Improving synaptic function in a mouse model of AD. *Cell*, **126**(4): 655–657.
- Latchman DS, Dent CL, Lillycrop KA, Wood JN. 1992. POU family transcription factors in sensory neurons. *Biochemical Society Transactions*, **20**(3): 627–631.
- Leyva-Díaz E, Masoudi N, Serrano-Saiz E, Glenwinkel L, Hobert O. 2020. Brn3/POU-IV-type POU homeobox genes-Paradigmatic regulators of neuronal identity across phylogeny. *WIREs Developmental Biology*, **9**(4): e374.
- Li Y, Schlamp CL, Poulsen KP, Nickells RW. 2000. Bax-dependent and independent pathways of retinal ganglion cell death induced by different damaging stimuli. *Experimental Eye Research*, **71**(2): 209–213.
- Lin YS, Kuo KT, Chen SK, Huang HS. 2018. Rbfox3/NEUN is dispensable for visual function. *PLoS One*, **13**(2): e0192355.
- Linden R, Perry VH. 1983. Massive retinotectal projection in rats. *Brain Research*, **272**(1): 145–149.
- Lingam S, Liu ZP, Yang BX, Wong W, Parikh BH, Ong JY, et al. 2021. cGMP-grade human iPSC-derived retinal photoreceptor precursor cells rescue cone photoreceptor damage in non-human primates. *Stem Cell Research & Therapy*, **12**(1): 464.
- Liu W, Khare SL, Liang X, Peters MA, Liu X, Cepko CL, et al. 2000. All Brn3 genes can promote retinal ganglion cell differentiation in the chick. *Development*, **127**(15): 3237–3247.
- Liu Y, Tapia ML, Yeh J, He RC, Pomerleu D, Lee RK. 2020. Differential Gamma-synuclein expression in acute and chronic retinal ganglion cell death in the retina and optic nerve. *Molecular Neurobiology*, **57**(2): 698–709.
- Liu ZP, Ilmarinen T, Tan GSW, Hongisto H, Wong EYM, Tsai ASH, et al. 2021. Submacular integration of hESC-RPE monolayer xenografts in a surgical non-human primate model. *Stem Cell Research & Therapy*, **12**(1): 423.
- Lopez AJ, Kim S, Qian XY, Rogers J, Stout JT, Thomasy SM, et al. 2022. Retinal organoids derived from rhesus macaque iPSCs undergo accelerated differentiation compared to human stem cells. *Cell Proliferation*, **55**(4): e13198.
- López-Herrera MPL, Mayor-Torroglosa S, De Imperial JM, Villegas-Pérez MP, Vidal-Sanz M. 2002. Transient ischemia of the retina results in altered retrograde axoplasmic transport: neuroprotection with brimonidine. *Experimental Neurology*, **178**(2): 243–258.
- Mali RS, Cheng M, Chintala SK. 2005. Intravitreal injection of a membrane depolarization agent causes retinal degeneration via matrix metalloproteinase-9. *Investigative Ophthalmology & Visual Science*, **46**(6): 2125–2132.
- Masin L, Claes M, Bergmans S, Cools L, Andries L, Davis BM, et al. 2021. A novel retinal ganglion cell quantification tool based on deep learning. *Scientific Reports*, **11**(1): 702.
- Matuszczak E, Tylicka M, Komarowska MD, Debek W, Hermanowicz A. 2020. Ubiquitin carboxy-terminal hydrolase L1 - physiology and pathology. *Cell Biochemistry and Function*, **38**(5): 533–540.
- May CA, Lütjen-Drecoll E, Narfström K. 2005. Morphological changes in the anterior segment of the Abyssinian cat eye with hereditary rod-cone degeneration. *Current Eye Research*, **30**(10): 855–862.
- Miesfeld JB, Ghiasvand NM, Marsh-Armstrong B, Marsh-Armstrong N, Miller EB, Zhang PF, et al. 2020. The *Atoh7* remote enhancer provides transcriptional robustness during retinal ganglion cell development. *Proceedings of the National Academy of Sciences of the United States of America*, **117**(35): 21690–21700.
- Miller DA, Grannonico M, Liu MN, Kuranov RV, Netland PA, Liu XR, et al. 2020. Visible-light optical coherence tomography fibergraphy for quantitative imaging of retinal ganglion cell axon bundles. *Translational Vision Science & Technology*, **9**(11): 11.
- Mu XQ, Beremand PD, Zhao S, Pershad R, Sun HX, Scarpa A, et al. 2004. Discrete gene sets depend on POU domain transcription factor Brn3b/Brn-3.2/POU4f2 for their expression in the mouse embryonic retina. *Development*, **131**(6): 1197–1210.
- Mullen RJ, Buck CR, Smith AM. 1992. NEUN, a neuronal specific nuclear protein in vertebrates. *Development*, **116**(1): 201–211.
- Munaut C, Lambert V, Noël A, Frankenne F, Deprez M, Foidart JM, et al. 2001. Presence of oestrogen receptor type  $\beta$  in human retina. *The British Journal of Ophthalmology*, **85**(7): 877–882.
- Muzyka VV, Brooks M, Badea TC. 2018. Postnatal developmental dynamics of cell type specification genes in BRN3A/Pou4f1 Retinal Ganglion Cells. *Neural Development*, **13**(1): 15.
- Nadal-Nicolás FM, Jiménez-López M, Salinas-Navarro M, Sobrado-Calvo P, Alburquerque-Béjar JJ, Vidal-Sanz M, et al. 2012. Whole number, distribution and co-expression of brn3 transcription factors in retinal ganglion cells of adult albino and pigmented rats. *PLoS One*, **7**(11): e49830.
- Nadal-Nicolás FM, Jiménez-López M, Salinas-Navarro M, Sobrado-Calvo P, Vidal-Sanz M, Agudo-Barriuso M. 2017. Microglial dynamics after axotomy-induced retinal ganglion cell death. *Journal of Neuroinflammation*, **14**(1): 218.
- Nadal-Nicolás FM, Jiménez-López M, Sobrado-Calvo P, Nieto-López L, Cánovas-Martínez I, Salinas-Navarro M, et al. 2009. Brn3a as a marker of retinal ganglion cells: qualitative and quantitative time course studies in naive and optic nerve-injured retinas. *Investigative Ophthalmology & Visual Science*, **50**(8): 3860–3868.
- Nadal-Nicolás FM, Madeira MH, Salinas-Navarro M, Jiménez-López M, Galindo-Romero C, Ortín-Martínez A, et al. 2015a. Transient downregulation of melanopsin expression after retrograde tracing or optic nerve injury in adult rats. *Investigative Ophthalmology & Visual Science*,

56(8): 4309–4323.

- Nadal-Nicolás FM, Miyagishima KJ, Li W. 2022. In search for the "idyllic" animal model to evaluate ocular pathologies and translate new therapies to improve human health. *Neural Regeneration Research*, **17**(12): 2697–2699.
- Nadal-Nicolás FM, Salinas-Navarro M, Jiménez-López M, Sobrado-Calvo P, Villegas-Pérez MP, Vidal-Sanz M, et al. 2014. Displaced retinal ganglion cells in albino and pigmented rats. *Frontiers in Neuroanatomy*, **8**: 99.
- Nadal-Nicolás FM, Salinas-Navarro M, Vidal-Sanz M, Agudo-Barriuso M. 2015b. Two methods to trace retinal ganglion cells with fluorogold: from the intact optic nerve or by stereotactic injection into the optic tract. *Experimental Eye Research*, **131**: 12–19.
- Nadal-Nicolás FM, Sobrado-Calvo P, Jiménez-López M, Vidal-Sanz M, Agudo-Barriuso M. 2015c. Long-term effect of optic nerve axotomy on the retinal ganglion cell layer. *Investigative Ophthalmology & Visual Science*, **56**(10): 6095–6112.
- Nguyen JV, Soto I, Kim KY, Bushong EA, Oglesby E, Valiente-Soriano FJ, et al. 2011. Myelination transition zone astrocytes are constitutively phagocytic and have synuclein dependent reactivity in glaucoma. *Proceedings of the National Academy of Sciences of the United States of America*, **108**(3): 1176–1181.
- Nilsson J, Gobom J, Sjödin S, Brinkmalm G, Ashton NJ, Svensson J, et al. 2021. Cerebrospinal fluid biomarker panel for synaptic dysfunction in Alzheimer's disease. *Alzheimer's & Dementia*, **13**(1): e12179.
- Nixon RA, Lewis SE, Dahl D, Marotta CA, Dräger UC. 1989. Early posttranslational modifications of the three neurofilament subunits in mouse retinal ganglion cells: neuronal sites and time course in relation to subunit polymerization and axonal transport. *Molecular Brain Research*, **5**(2): 93–108.
- Norte-Muñoz M, Lucas-Ruiz F, Gallego-Ortega A, García-Bernal D, Valiente-Soriano FJ, De La Villa P, Vidal-Sanz M, et al. 2021. Neuroprotection and axonal regeneration induced by bone marrow mesenchymal stromal cells depend on the type of transplant. *Frontiers in Cell and Developmental Biology*, **9**: 772223.
- Onishi A, Peng GH, Poth EM, Lee DA, Chen JC, Alexis U, et al. 2010. The orphan nuclear hormone receptor *ERRβ* controls rod photoreceptor survival. *Proceedings of the National Academy of Sciences of the United States of America*, **107**(25): 11579–11584.
- Pan L, Yang ZY, Feng L, Gan L. 2005. Functional equivalence of Brn3 POU-domain transcription factors in mouse retinal neurogenesis. *Development*, **132**(4): 703–712.
- Parmhans N, Fuller AD, Nguyen E, Chuang K, Swygart D, Wienbar SR, et al. 2021. Identification of retinal ganglion cell types and brain nuclei expressing the transcription factor Brn3c/Pou4f3 using a Cre recombinase knock-in allele. *The Journal of Comparative Neurology*, **529**(8): 1926–1953.
- Parrilla-Reverter G, Agudo M, Nadal-Nicolás F, Alarcón-Martínez L, Jiménez-López M, Salinas-Navarro M, et al. 2009. Time-course of the retinal nerve fibre layer degeneration after complete intra-orbital optic nerve transection or crush: a comparative study. *Vision Research*, **49**(23): 2808–2825.
- Pereiro X, Ruzafa N, Urcola JH, Sharma SC, Vecino E. 2020. Differential distribution of RBPMS in pig, rat, and human retina after damage. *International Journal of Molecular Sciences*, **21**(23): 9330.
- Piccinini M, Merighi A, Bruno R, Cascio P, Curto M, Mioletti SC, et al. 1996. Affinity purification and characterization of protein gene product 9.5 (PGP9.5) from retina. *The Biochemical Journal*, **318**(Pt 2): 711–716.
- Plaza S, Hennemann H, Möröy T, Saule S, Dozier C. 1999. Evidence that POU factor Brn-3B regulates expression of Pax-6 in neuroretina cells. *Journal of Neurobiology*, **41**(3): 349–358.
- Provencio I, Rodriguez IR, Jiang GS, Hayes WP, Moreira EF, Rollag MD. 2000. A novel human opsin in the inner retina. *The Journal of Neuroscience*, **20**(2): 600–605.
- Quan MZ, Kosaka J, Watanabe M, Wakabayashi T, Fukuda Y. 1999. Survival of axotomized retinal ganglion cells in peripheral nerve-grafted ferrets. *Investigative Ophthalmology & Visual Science*, **40**(10): 2360–2366.
- Raymond ID, Pool AL, Vila A, Brecha NC. 2009. A *Thy1*-CFP DBA/2J mouse line with cyan fluorescent protein expression in retinal ganglion cells. *Visual Neuroscience*, **26**(5–6): 453–465.
- Raymond ID, Vila A, Huynh UC, Brecha NC. 2008. Cyan fluorescent protein expression in ganglion and amacrine cells in a *thy1*-CFP transgenic mouse retina. *Molecular Vision*, **14**: 1559–1574.
- Real MA, Heredia R, Dávila JC, Guirado S. 2008. Efferent retinal projections visualized by immunohistochemical detection of the estrogen-related receptor beta in the postnatal and adult mouse brain. *Neuroscience Letters*, **438**(1): 48–53.
- Rheaume BA, Jereen A, Bolisetty M, Sajid MS, Yang Y, Renka K, et al. 2018. Single cell transcriptome profiling of retinal ganglion cells identifies cellular subtypes. *Nature Communications*, **9**(1): 2759.
- Rodieck RW. 1979. Visual pathways. *Annual Review of Neuroscience*, **2**: 193–225.
- Rodríguez AR, De Sevilla Müller LP, Brecha NC. 2014. The RNA binding protein RBPMS is a selective marker of ganglion cells in the mammalian retina. *The Journal of Comparative Neurology*, **522**(6): 1411–1443.
- Romero-Alemán MM, Monzón-Mayor M, Santos E, Lang DM, Yanes C. 2012. Neuronal and glial differentiation during lizard (*Gallotia galloti*) visual system ontogeny. *The Journal of Comparative Neurology*, **520**(10): 2163–2184.
- Romero-Alemán MM, Monzón-Mayor M, Santos E, Yanes C. 2010. Expression of neuronal markers, synaptic proteins, and glutamine synthetase in the control and regenerating lizard visual system. *The Journal of Comparative Neurology*, **518**(19): 4067–4087.
- Ruiz-Ederra J, García M, Hicks D, Vecino E. 2004. Comparative study of the three neurofilament subunits within pig and human retinal ganglion cells. *Molecular Vision*, **10**: 83–92.
- Ruzafa N, Rey-Santano C, Mielgo V, Pereiro X, Vecino E. 2017. Effect of hypoxia on the retina and superior colliculus of neonatal pigs. *PLoS One*, **12**(4): e0175301.
- Sajgo S, Ghinia MG, Brooks M, Kretschmer F, Chuang K, Hiriyanna S, et al. 2017. Molecular codes for cell type specification in Brn3 retinal ganglion cells. *Proceedings of the National Academy of Sciences of the United States of America*, **114**(20): E3974–E3983.
- Salinas-Navarro M, Alarcón-Martínez L, Valiente-Soriano FJ, Jiménez-López M, Mayor-Torroglosa S, Avilés-Trigueros M, et al. 2010. Ocular hypertension impairs optic nerve axonal transport leading to progressive retinal ganglion cell degeneration. *Experimental Eye Research*, **90**(1): 168–183.
- Salinas-Navarro M, Jiménez-López M, Valiente-Soriano FJ, Alarcón-Martínez L, Avilés-Trigueros M, Mayor S, et al. 2009a. Retinal ganglion cell population in adult albino and pigmented mice: a computerized analysis of the entire population and its spatial distribution. *Vision Research*, **49**(6): 637–647.
- Salinas-Navarro M, Mayor-Torroglosa S, Jiménez-López M, Avilés-Trigueros M, Holmes TM, Lund RD, et al. 2009b. A computerized analysis

- of the entire retinal ganglion cell population and its spatial distribution in adult rats. *Vision Research*, **49**(1): 115–126.
- Sánchez-Migallón MC, Nadal-Nicolás FM, Jiménez-López M, Sobrado-Calvo P, Vidal-Sanz M, Agudo-Barriuso M. 2011. Brain derived neurotrophic factor maintains Brn3a expression in axotomized rat retinal ganglion cells. *Experimental Eye Research*, **92**(4): 260–267.
- Sánchez-Migallón MC, Valiente-Soriano FJ, Nadal-Nicolás FM, Di Pierdomenico J, Vidal-Sanz M, Agudo-Barriuso M. 2018a. Survival of melanopsin expressing retinal ganglion cells long term after optic nerve trauma in mice. *Experimental Eye Research*, **174**: 93–97.
- Sánchez-Migallón MC, Valiente-Soriano FJ, Nadal-Nicolás FM, Vidal-Sanz M, Agudo-Barriuso M. 2016. Apoptotic retinal ganglion cell death after optic nerve transection or crush in mice: delayed RGC loss with BDNF or a caspase 3 inhibitor. *Investigative Ophthalmology & Visual Science*, **57**(1): 81–93.
- Sánchez-Migallón MC, Valiente-Soriano FJ, Salinas-Navarro M, Nadal-Nicolás FM, Jiménez-López M, Vidal-Sanz M, et al. 2018b. Nerve fibre layer degeneration and retinal ganglion cell loss long term after optic nerve crush or transection in adult mice. *Experimental Eye Research*, **170**: 40–50.
- Sanes JR, Masland RH. 2015. The types of retinal ganglion cells: current status and implications for neuronal classification. *Annual Review of Neuroscience*, **38**: 221–246.
- Santos E, Romero-Alemán MM, Monzón-Mayor M, Yanes C. 2014. Variable functional recovery and minor cell loss in the ganglion cell layer of the lizard *Gallotia galloti* after optic nerve axotomy. *Experimental Eye Research*, **118**: 89–99.
- Sasaoka M, Taniguchi T, Shimazawa M, Ishida N, Shimazaki A, Hara H. 2006. Intravitreal injection of endothelin-1 caused optic nerve damage following to ocular hypoperfusion in rabbits. *Experimental Eye Research*, **83**(3): 629–637.
- Sato T, Hamaoka T, Aizawa H, Hosoya T, Okamoto H. 2007. Genetic single-cell mosaic analysis implicates ephrinB2 reverse signaling in projections from the posterior tectum to the hindbrain in zebrafish. *The Journal of Neuroscience*, **27**(20): 5271–5279.
- Schiller PH. 1986. The central visual system. *Vision Research*, **26**(9): 1351–1386.
- Schlamp CL, Johnson EC, Li Y, Morrison JC, Nickells RW. 2001. Changes in Thy1 gene expression associated with damaged retinal ganglion cells. *Molecular Vision*, **7**: 192–201.
- Schmidt TM, Chen SK, Hattar S. 2011. Intrinsically photosensitive retinal ganglion cells: many subtypes, diverse functions. *Trends in Neurosciences*, **34**(11): 572–580.
- Sefton AJ, Lam K. 1984. Quantitative and morphological studies on developing optic axons in normal and enucleated albino rats. *Experimental Brain Research*, **57**(1): 107–117.
- Sellés-Navarro I, Villegas-Pérez MP, Salvador-Silva M, Ruiz-Gómez JM, Vidal-Sanz M. 1996. Retinal ganglion cell death after different transient periods of pressure-induced ischemia and survival intervals. A quantitative in vivo study. *Investigative Ophthalmology & Visual Science*, **37**(10): 2002–2014.
- Serrano-Saiz E, Leyva-Díaz E, De La Cruz E, Hobert O. 2018. BRN3-type POU homeobox genes maintain the identity of mature postmitotic neurons in nematodes and mice. *Current Biology*, **28**(17): 2813–2823.e2.
- Setsuie R, Wada K. 2007. The functions of UCH-L1 and its relation to neurodegenerative diseases. *Neurochemistry International*, **51**(2–4): 105–111.
- Sheng WL, Weng SJ, Li F, Zhang Y, He QX, Sheng WX, et al. 2021. Immunohistological Localization of Mel1a Melatonin Receptor in Pigeon Retina. *Nature and Science of Sleep*, **13**: 113–121.
- Siddiqui AM, Sabljic TF, Koeberle PD, Ball AK. 2014. Downregulation of BM88 after optic nerve injury. *Investigative Ophthalmology & Visual Science*, **55**(3): 1919–1929.
- Simmons AB, Bloomsburg SJ, Billingslea SA, Merrill MM, Li S, Thomas MW, et al. 2016. *Pou4f2* knock-in Cre mouse: a multifaceted genetic tool for vision researchers. *Molecular Vision*, **22**: 705–717.
- Smith MD, Dawson SJ, Latchman DS, Boxer LM. 1998. The N-terminal domain unique to the long form of the Brn-3a transcription factor is essential to protect neuronal cells from apoptosis and for the activation of Bcl-2 gene expression. *Nucleic Acids Research*, **26**(18): 4100–4107.
- Surgucheva I, Weisman AD, Goldberg JL, Shnyra A, Surguchov A. 2008.  $\gamma$ -synuclein as a marker of retinal ganglion cells. *Molecular Vision*, **14**: 1540–1548.
- Takemura Y, Ojima H, Oshima G, Shinoda M, Hasegawa Y, Kitago M, et al. 2021. Gamma-synuclein is a novel prognostic marker that promotes tumor cell migration in biliary tract carcinoma. *Cancer Medicine*, **10**(16): 5599–5613.
- Tapia ML, Nascimento-Dos-Santos G, Park KK. 2022. Subtype-specific survival and regeneration of retinal ganglion cells in response to injury. *Frontiers in Cell and Developmental Biology*, **10**: 956279.
- Telegina DV, Kolosova NG, Kozhevnikova OS. 2019. Immunohistochemical localization of NGF, BDNF, and their receptors in a normal and AMD-like rat retina. *BMC Medical Genomics*, **12**(Suppl 2): 48.
- Thanos S, Vidal-Sanz M, Aguayo AJ. 1987. The use of rhodamine-B-isothiocyanate (RITC) as an anterograde and retrograde tracer in the adult rat visual system. *Brain Research*, **406**(1–2): 317–321.
- Tran NM, Shekhar K, Whitney IE, Jacobi A, Benhar I, Hong GS, et al. 2019. Single-cell profiles of retinal ganglion cells differing in resilience to injury reveal neuroprotective genes. *Neuron*, **104**(6): 1039–1055.e12.
- Triplett JW, Wei W, Gonzalez C, Sweeney NT, Huberman AD, Feller MB, et al. 2014. Dendritic and axonal targeting patterns of a genetically-specified class of retinal ganglion cells that participate in image-forming circuits. *Neural Development*, **9**(1): 2.
- Trowern AR, Laight R, MacLean N, Mann DA. 1996. Detection of neuron-specific protein gene product (PGP) 9.5 in the rat and zebrafish using anti-human PGP9.5 antibodies. *Neuroscience Letters*, **210**(1): 21–24.
- Ünal-Çevik I, Kılınç M, Gürsoy-Özdemir Y, Gurer G, Dalkara T. 2004. Loss of NEUN immunoreactivity after cerebral ischemia does not indicate neuronal cell loss: a cautionary note. *Brain Research*, **1015**(1–2): 169–174.
- Valiente-Soriano FJ, García-Ayuso D, Ortín-Martínez A, Jiménez-López M, Galindo-Romero C, Villegas-Pérez MP, et al. 2014. Distribution of melanopsin positive neurons in pigmented and albino mice: evidence for melanopsin interneurons in the mouse retina. *Frontiers in Neuroanatomy*, **8**: 131.
- Valiente-Soriano FJ, Salinas-Navarro M, Jiménez-López M, Alarcón-Martínez I, Ortín-Martínez A, Bernal-Garro JM, et al. 2015. Effects of ocular hypertension in the visual system of pigmented mice. *PLoS One*, **10**(3): e0121134.
- Van Nassauw L, Wu M, De Jonge F, Adriaensens D, Timmermans JP. 2005. Cytoplasmic, but not nuclear, expression of the neuronal nuclei (NeuN) antibody is an exclusive feature of Dogiel type II neurons in the guinea-pig gastrointestinal tract. *Histochemistry and Cell Biology*, **124**(5): 369–377.
- Vickers JC, Costa M. 1992. The neurofilament triplet is present in distinct

- subpopulations of neurons in the central nervous system of the guinea-pig. *Neuroscience*, **49**(1): 73–100.
- Vickers JC, Riederer BM, Marugg RA, Buée-Scherrer V, Buée L, Delacourte A, et al. 1994. Alterations in neurofilament protein immunoreactivity in human hippocampal neurons related to normal aging and Alzheimer's disease. *Neuroscience*, **62**(1): 1–13.
- Vidal-Sanz M, Galindo-Romero C, Valiente-Soriano FJ, Nadal-Nicolás FM, Ortín-Martínez A, Rovere G, et al. 2017. Shared and differential retinal responses against optic nerve injury and ocular hypertension. *Frontiers in Neuroscience*, **11**: 235.
- Vidal-Sanz M, Salinas-Navarro M, Nadal-Nicolás FM, Alarcón-Martínez L, Valiente-Soriano FJ, De Imperial JM, et al. 2012. Understanding glaucomatous damage: anatomical and functional data from ocular hypertensive rodent retinas. *Progress in Retinal and Eye Research*, **31**(1): 1–27.
- Vidal-Sanz M, Valiente-Soriano FJ, Ortín-Martínez A, Nadal-Nicolás FM, Jiménez-López M, Salinas-Navarro M, et al. 2015. Retinal neurodegeneration in experimental glaucoma. *Progress in Brain Research*, **220**: 1–35.
- Vidal-Sanz M, Villegas-Pérez MP, Bray GM, Aguayo AJ. 1988. Persistent retrograde labeling of adult rat retinal ganglion cells with the carbocyanine dye dil. *Experimental Neurology*, **102**(1): 92–101.
- Villegas-Pérez MP, Vidal-Sanz M, Rasminsky M, Bray GM, Aguayo AJ. 1993. Rapid and protracted phases of retinal ganglion cell loss follow axotomy in the optic nerve of adult rats. *Journal of Neurobiology*, **24**(1): 23–36.
- Völggi B, Bloomfield SA. 2002. Axonal neurofilament-H immunolabeling in the rabbit retina. *The Journal of Comparative Neurology*, **453**(3): 269–279.
- Wakabayashi T, Fukuda Y, Kosaka J. 1996a. Monoclonal antibody C38 labels surviving retinal ganglion cells after peripheral nerve graft in axotomized rat retina. *Brain Research*, **725**(1): 121–124.
- Wakabayashi T, Fukuda Y, Kosaka J. 1996b. Monoclonal antibody C38 recognizes retinal ganglion cells in cats and rats. *Vision Research*, **36**(8): 1081–1090.
- Wakabayashi T, Kosaka J, Mochii M, Miki Y, Mori T, Takamori Y, et al. 2010. C38, equivalent to BM88, is developmentally expressed in maturing retinal neurons and enhances neuronal maturation. *Journal of Neurochemistry*, **112**(5): 1235–1248.
- Wang HH, Gallagher SK, Byers SR, Madl JE, Gionfriddo JR. 2015. Retinal ganglion cell distribution and visual acuity in alpacas (*Vicugna pacos*). *Veterinary Ophthalmology*, **18**(1): 35–42.
- Wang YL, Wang WY, Liu J, Huang X, Liu RX, Xia HK, et al. 2016. Protective effect of ala in crushed optic nerve cat retinal ganglion cells using a new marker RBPMS. *PLoS One*, **11**(8): e0160309.
- Wilkinson KD, Deshpande S, Larsen CN. 1992. Comparisons of neuronal (PGP 9.5) and non-neuronal ubiquitin C-terminal hydrolases. *Biochemical Society Transactions*, **20**(3): 631–637.
- Xiang M, Zhou L, Macke JP, Yoshioka T, Hendry SH, Eddy RL, et al. 1995. The Brn-3 family of POU-domain factors: primary structure, binding specificity, and expression in subsets of retinal ganglion cells and somatosensory neurons. *The Journal of Neuroscience*, **15**(7 Pt 1): 4762–4785.
- Xiao X, Zhao TT, Miyagishima KJ, Chen S, Li W, Nadal-Nicolás FM. 2021. Establishing the ground squirrel as a superb model for retinal ganglion cell disorders and optic neuropathies. *Laboratory Investigation*, **101**(9): 1289–1303.
- Xu MY, Pang QQ, Xu SQ, Ye CY, Lei R, Shen YC, et al. 2018. Hypoxia-inducible factor-1 $\alpha$  activates transforming growth factor- $\beta$ 1/Smad signaling and increases collagen deposition in dermal fibroblasts. *Oncotarget*, **9**(3): 3188–3197.
- Zhang J, Huo YB, Yang JL, Wang XZ, Yan BY, Du XH, et al. 2022. Automatic counting of retinal ganglion cells in the entire mouse retina based on improved YOLOv5. *Zoological Research*, **43**(5): 738–749.
- Zhang XM, Liu DTL, Chiang SWY, Choy KW, Pang CP, Lam DSC, et al. 2010. Immunopanning purification and long-term culture of human retinal ganglion cells. *Molecular Vision*, **16**: 2867–2872.
- Zhou JX, Liu YJ, Chen X, Zhang X, Xu J, Yang K, et al. 2018. Low-Intensity pulsed ultrasound protects retinal ganglion cell from optic nerve injury induced apoptosis via YES associated protein. *Frontiers in Cellular Neuroscience*, **12**: 160.